Title
Human Intestinal Spheroids cultured using Sacrificial Micromolding as a Model System for Studying Drug Transport

Author
Samy, Karen

Publication Date
2019

Peer reviewed|Thesis/dissertation

Human Intestinal Spheroids cultured using Sacrificial Micromolding as a Model System for Studying Drug Transport

by

Karen Samy

A dissertation submitted in partial satisfaction of the

requirements for the degree of

Joint Doctor of Philosophy
with University of California San Francisco

in

Bioengineering

in the

Graduate Division

of the

University of California, Berkeley

Committee in charge:

Professor Tejal Desai, Chair
Professor Dorian Liepmann
Professor Gregory Aponte

Summer 2019

Human Intestinal Spheroids cultured using Sacrificial Micromolding as a Model System for Studying Drug Transport

Abstract

Human Intestinal Spheroids cultured using Sacrificial Micromolding as a Model System for Studying Drug Transport

by

Karen Samy

Doctor of Philosophy in Bioengineering

University of California, Berkeley

Professor Tejal Desai, Chair

In vitro cell culture models have proven to be essential in early drug discovery and drug development to predict *in vivo* drug responses. More specifically, *in vitro* models of the small intestine are crucial tools for the prediction of drug absorption. The Caco-2 monolayer transwell model has been widely employed to assess drug absorption across the intestine. However, it is now well-established that 3D *in vitro* models capture tissue-specific architecture and interactions with the extracellular matrix and therefore better recapitulate the complex *in vivo* environment.

We develop a novel Sacrificial Micromolding technique to culture geometrically controlled self-assembling lumenized and polarized Caco-2 spheroids in a three-dimensional matrix. Compared to other techniques, this Sacrificial Micromolding technique allows for precise control of size, shape as well as location of spheroids within a gel matrix. In addition, it does not expose the spheroids to unnecessary sheer stress that could alter the cellular phenotype. We further characterize the intestinal spheroids for correct polarization, barrier properties and changes in gene expression and transporter function compared to 2D monolayers. We report that the spheroids display reproducible intestinal features and functions that are more representative of the *in vivo* small intestine than the widely used 2D transwell model. We also show that Caco-2 cell maturation and differentiation into the intestinal epithelial phenotype occur faster in spheroids and that they are viable for a longer period of time.

To overcome the limitation of lacking access to the luminal space of these spheroids, we exploit our three-dimensional patterning expertise as well as the directed epithelial self-organization to develop a technique to non-intrusively incorporate polymeric microparticles into the reconstituted intestinal spheroids. These polymeric microparticles can act as carriers or sensors to instruct or characterize tissue biology for *in vitro* assays. We use this technique to further study how microparticles of different shape and size as well as different compositions affect the self-organization and lumenization process of these tissues. We also develop a novel pH sensitive microsensor that can measure the luminal pH of reconstituted epithelial microtissues.

We found that spherical microparticles that are 30 µm in diameter do not affect the self-organization process and are efficient at localizing to the lumen. Interestingly, we found that adhesive microparticles like polystyrene perturbed the self-organization and lumen formation and led to tissue inversion. Finally, we used this finding to invert the polarity of the spheroids by culturing them around Matrigel beads allowing superficial access to the apical membrane and making our intestinal spheroid model more physiological.

These studies offer a novel approach for investigating luminal microenvironments and drug-delivery across epithelial barriers without affecting the self-organization of the tissues. We believe that using Sacrificial Micromolding we developed a robust and reproducible *in vitro* intestinal model that could serve as a valuable system to expedite drug screening as well as to study intestinal transporter function.

To Rami Botros

For teaching me to think critically and the importance of good philosophy

Contents

List of Figures

List of Tables

Acknowledgments

I would not have been able to complete my PhD without the support of many people. My advisor, Prof. Tejal Desai has allowed me to freely pursue my research interests and provided many opportunities for growth including conferences, talks, and meetings as well as networking opportunities with industry. Tejal has encouraged me to pursue a three-month summer internship at Genentech to explore research in industry and has been supportive of my future goals and aspirations no matter what they were. I am grateful to her for providing me with a relatively stress-free five years.

I would also like to acknowledge the National Science Foundation (NSF) and the Berkeley Chancellor's Fellowship and the International Foundation for Ethical Research (IFER) for grant funding and support. Special thanks to Dr. Alec Cerchiari, Dr. Erica Schlesinger and Dr. Jean Kim who were great mentors as I began my PhD.

I am grateful to the Desai lab and my colleagues and friends Priya Mohindra, Gauree Chendke, Long Le, William Lykins, Yiqi Cao, Cameron Nemeth, and Joel Finbloom for providing a lab environment that allowed me to happily go into lab everyday knowing that I will get all the help and support I needed and that I could count on them to cheer me up if experiments did not go as planned. I had fun times with the Desai lab from wine and cheese nights to karaoke nights to weekend brunches and more.

I would especially like to thank my colleague and friend Elizabeth Levy. Liz and I have worked together on projects for the past two years in the lab. It has been of tremendous value to me to work alongside someone as smart and diligent as Liz who always wanted to produce high quality and well-thought-out work. More importantly, Liz had an astounding ability to read my mind as soon as I came into lab every day and working with her has been the smoothest and most enjoyable collaboration I have had. I am grateful for her thoughtful gifts and for all our Starbucks coffee runs where she patiently listened to my problems. I am grateful to her for being a kindhearted friend and for giving me an enjoyable lab experience.

I would also like to thank my colleague and friend Colin Zamecnik. Colin has been my unofficial mentor and friend throughout my PhD. His guidance in planning and troubleshooting experiments has helped me grow as a scientist. He has been an essential part of the lab and a great and helpful friend to talk to about problems. I owe him my successful PhD and my limited knowledge of immunology.

My Bioengineering friends, Jonathon Muncie, Allison Drain, Roberto Falcon-Banchs, David Monteiro, Courtney Mazur and Nick Smith have been an irreplaceable pillar of support. I am grateful to Jon for being a caring friend and the life of the group, Allison for the insightful discussions and for sharing our feelings over beer, Roberto for his perspective on how to live, Dave for making me laugh, Courtney for keeping my sugar levels high and Nick for political discussions. I am grateful to all of them for filling my five years with happiness and laughter.

I would also like to thank my longtime friend Rami Botros. Rami has been my friend and teacher since my first year of college. He has taught me everything from college calculus to biomechanics to coding, analyzing data and making good powerpoint slides. More

importantly, Rami has been the reason I still believed in myself as a scientist. He helped me get over my imposter syndrome by constantly pointing out my strengths and skills. Aside from science, he has helped me grow as a person and develop opinions through intriguing and challenging philosophical discussions. I am grateful to him for believing in me and for the lifelong learning.

I am grateful to my parents for doing everything they can to move to the USA so that my sister and I can have a good education. I would not have this degree without their sacrifices and their support. They have taught me the value of hard work and dedication. Their valuing and appreciation of science and education has shaped my interests and views and my desire to pursue a PhD. I am grateful to them for setting the best example.

I am grateful to my sister for being my role model and allowing me to learn from her mistakes and giving me advice on how to be a successful PhD student. My sister has been the one making the big steps and taking the risks which enabled me to follow in her footsteps making my experience much easier.

I am lucky to have been a member of the UCB-UCSF Joint Program in Bioengineering and the Bioengineering Association of Students (BEAST). I have met incredibly smart and fun people and this program has provided me with a collaborative academic and social community. The bay area has been a fantastic place to complete my doctoral studies and build my network for my future career. I have truly enjoyed my five years in graduate school and made amazing lifelong friends.

Chapter 1

Sacrificial Micromolding as a Novel Technique for Culturing Intestinal Spheroids

1.1 Introduction

Two-dimensional (2D) *in vitro* cell culture models that are cultured on planar substrates have been used for several decades in drug discovery and drug development to predict *in vivo* drug responses. However, because of the lack of tissue specific architecture as well as cell-cell and cell-extracellular matrix (ECM) interactions, cell behaviors and morphologies can be vastly different from what is observed *in vivo*. In addition to biochemical signals, structural and mechanical cues have proven to have a profound impact on cellular phenotype. In the past decade, advances in cell biology as well as the rise of microfabrication technologies and tissue engineering has led to the rise of three-dimensional (3D) cell culture systems that have materialized as a more biomimetic tool in early drug discovery.[21] These models have become the new gold standard *in vitro* models for recapitulating *in vivo* phenotype of cells and tissues and have resulted in more accurate predictions of drug responses to disease. For example, colon cancer HCT-116 cells have been found to be more resistant to anticancer drugs such as melphalan, fluorouracil, and irinotecan in 3D culture compared to 2D culture which is consistent with observations *in vivo*.[33] Moreover, 3D cell culture models have the advantage of not only enabling drug safety and efficacy assessment in a more *in vivo*-like context but they also eliminate the species differences observed between humans and animals that often impede interpretation of preclinical outcomes by allowing drug testing directly in human systems. Additionally, using these models can cut the cost of screening by as much as 90% and can save weeks if not months of tedious work.[36]

In 3D cell culture models, cells are seeded on top of or within polymeric scaffolds that support the growth or differentiation of the cells into 3D spheroids that mimic many features and functions of the tissues they are derived from. This spheroid model has many advantages

compared to monolayer cultures. Spheroids have a well-defined geometry and architecture as well as physiological cell-ell and cell-ECM interactions. Additionally, they are able to develop and capture gradients of nutrients and oxygen as well as soluble signals.[21] However, previously used techniques of culturing spheroids such as low-adhesion plates, hanging drop plates or spinner flasks used to promote the self-aggregation of cells into spheroids[21] have many disadvantages including subjecting spheroids to shear stress and the lack of 3D geometric constraints to the reconstituted cells that, therefore, lead to heterogeneous tissues in terms of size, shape, and position within a gel.

1.2 Sacrificial Micromolding

Photolithography techniques derived from the semiconductor industry are commonly used to constrain 3D tissues by patterning or replica-molding scaffolds that can accommodate cells at high density within a predefined geometrical structure.[32][35] The materials typically used in this approach are those that can be readily patterned by photolithography (e.g., epoxy-based photoresists and UV-reactive polymers) or micromolded by soft lithography (e.g., elastomers and agarose). For example, polydimethylsiloxane (PDMS), agarose, or poly (ethylene glycol) (PEG) microwells provide semi-3D (or 2.5D) cell culture platforms that produce complex tissue geometries at low cost and high throughput.[16][27][34] Unfortunately, these materials do not recapitulate the physicochemical properties of the *in vivo* ECM. Elaboration of these photolithographic approaches allowed the formation of spatially and geometrically defined 3D cellular patterns within biomimetic ECM gels. Microcavities within type I collagen gels have been seeded with cells and overlaid with additional collagen to gain control over the geometry and spatial organization of 3D tissues within an ECM.[43] However, this strategy becomes challenging with other soft ECM gels like the laminin-rich reconstituted basement membrane hydrogel known as Matrigel. Matrigel mimics the basement membrane *in vivo* in its multifactorial composition of matrix components including laminin, collagen IV, entactin etc., as well as in its mechanical properties that promote tissue morphogenesis and allow diffusion of biochemical factors and nutrients.[30][37] However, because of the gel's low stiffness and its time-dependent viscoelastic properties geometric patterning becomes a challenge.

To overcome this challenge, a combination of lithographic and molding techniques have been used to pattern islands of Matrigel on a glass substrate.[53] By controlling the cell density suspended in the liquid Matrigel molded against supports made out of PDMS, single cells can be deposited to grow into single tissues. However, precise control over cell number in each island is a challenge and this strategy lacks geometric and spatial control of multicellular architectures embedded within the gel.

We, therefore, sought an improved micromolding strategy for patterning cells into spatially and geometrically controlled multicellular structures fully embedded in Matrigel. Inspired by previous reports that used degradable materials such as agarose for patterning microfluidic channels embedded in collagen or fibrin[4][24], we envisioned using this material

as a degradable scaffold for micromolding spatially and geometrically resolved multicellular structures that can be transferred to soft biomimetic gels.

1.3 Culture of Intestinal Spheroids using Sacrificial Micromolding

We used Sacrificial Micromolding to culture geometrically and spatially controlled multicellular intestinal spheroids by allowing precise control over the initial size of the reconstituted cell aggregates.[15] Using simple photolithography and micromolding techniques, we fabricated PDMS stamps with 120 µm diameter pillars (Fig. 1.1). The PDMS stamps were deposited onto a 250 µl drop of 3% liquid agarose within the wells of a 24-well plate. Agarose gelation occured within minutes of placing the 24-well plate at room temperature. To form cell aggregates, the human colon adenocarcinoma cells (Caco-2) were dissociated from plates and centrifuged into the sacrificial agarose microwells and allowed to aggregate for 24 hours. The aggregates were then transferred to a Matrigel slab and incubated for 1 hour. Afterwards, an additional Matrigel layer was added on top of the cell aggregates before adding media for long-term culture. The aggregates were cultured in the Matrigel matrix for 5 additional days. Besides its ease of use, agarose was chosen for the sacrificial microwells to prevent cells from adhering to the microwells allowing easy transfer to the Matrigel matrix. Matrigel was chosen as the ECM for its unparalleled imitation of the basement membrane *in vivo* as well as its ability to form stable but soft gels (< 0.5 kPa)[54] that match soft tissues like the small intestine. These properties also allow Matrigel to promote cell morphogenesis as well as the diffusion of biochemical factors throughout the 3D matrix .

1.4 Cell Viability and Lumenization

We found that after 5 days in Matrigel, the Caco-2 cells self-organize into intestinal epithelial tissues with a confluent monolayer of cells surrounding a hollow lumen. A previous study showed that the number of lumen formed is a function of the diameter of the cell aggregates.[15] We found that with an aggregate diameter of 120 µm, out of a total of 1072 spheroids, 1012 of the spheroids formed a lumen after 6 days in culture as determined by confocal microscopy (n experiment =3; 477/504, 293/305, 242/263), yielding an average success rate of 94 %. Additionally, we show that the spheroids are amenable to long-term culture. The spheroids remained stable and viable in Matrigel for 21 days. Figure 1.2A shows spheroids that were cultured for 6 days, 10 days, 14 days and 21 days in Matrigel. The spheroids maintained their structure and remained lumenized with a monolayer of cells surrounding the hollow lumen. Cell viability was confirmed by conducting a live/dead staining assay after 21 days in culture (Fig. 1.2B) and only 1 ± 0.3 % of spheroids were determined to be dead using a propidium iodide stain. The ability of these spheroids to survive for 21 days in Matrigel increases the throughput of this system compared to the transwell system.

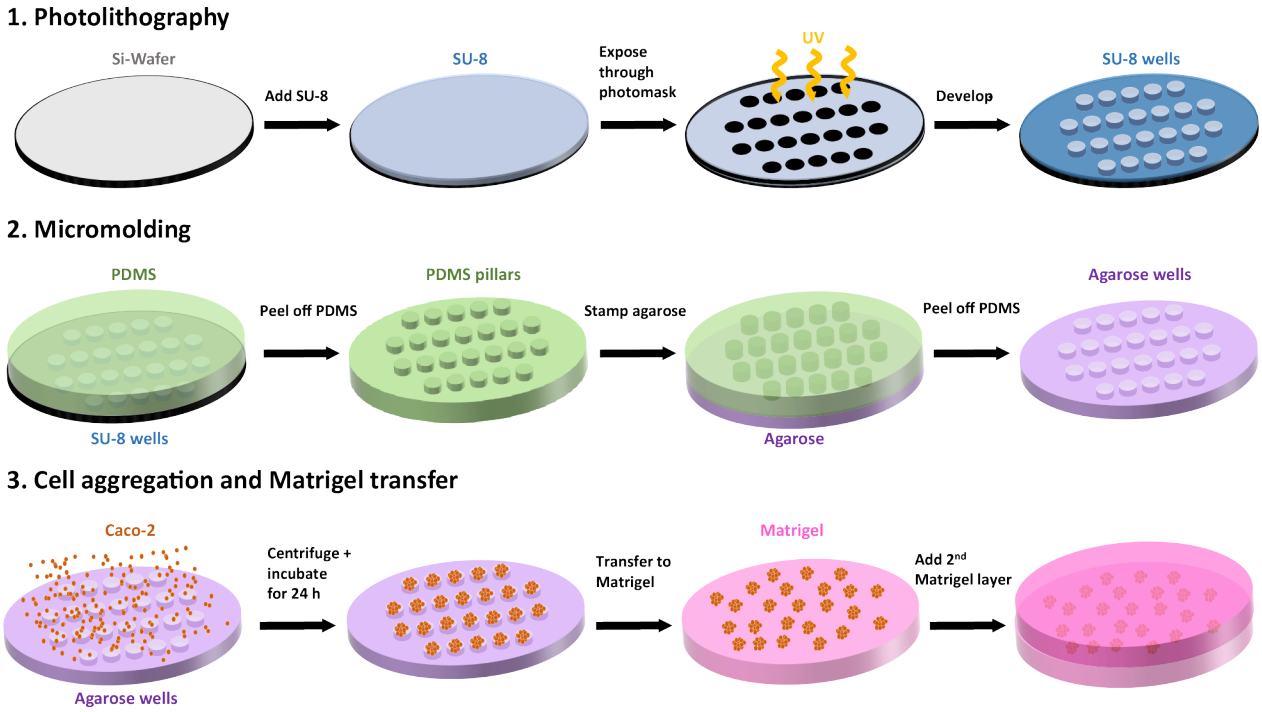

Figure 1.1: Culture of geometrically-controlled intestinal spheroids using Sacrificial Micromolding. Schematic representation of the formation and use of agarose micromolds for patterning Caco-2 spheroids in a soft Matrigel matrix.

1.5 Summary

The ability to reproduce highly complex tissues *in vitro* in a stable and reproducible manner is critical for the study and engineering of mammalian tissues. We developed a novel Sacrificial Micromolding technique that takes advantage of the non-adhesive properties of agarose to precisely define the initial size and geometry of intestinal spheroids fully embedded in a soft Matrigel gel. We found that using Sacrificial Micromolding, we can achieve homogeneous lumenized and confluent spheroids after only 6 days in culture. Furthermore, with an aggregate diameter of 120 µm we can achieve a 94% success rate of lumen formation. Additionally, we show that the spheroids are amenable to long-term culture and remain lumenized for 21 days. This increases the throughput of the system since it can be used for multiple assays. This technique captures the process of self-organization and has the potential of recapitulating heterotypic cellular interactions as well as cell-ECM interactions of more complex tissues.[15] The formulation of the gel could be optimized to promote distinct aspects of morphogenesis that characterize different tissue types. Additionally, this method can be extended to encapsulate aggregates within a spectrum of hydrogel-based scaffolds currently under development to bypass the complexity and variability of Matrigel. Given the flexibility of the technique, we anticipate that Sacrificial Micromolding will find utility in

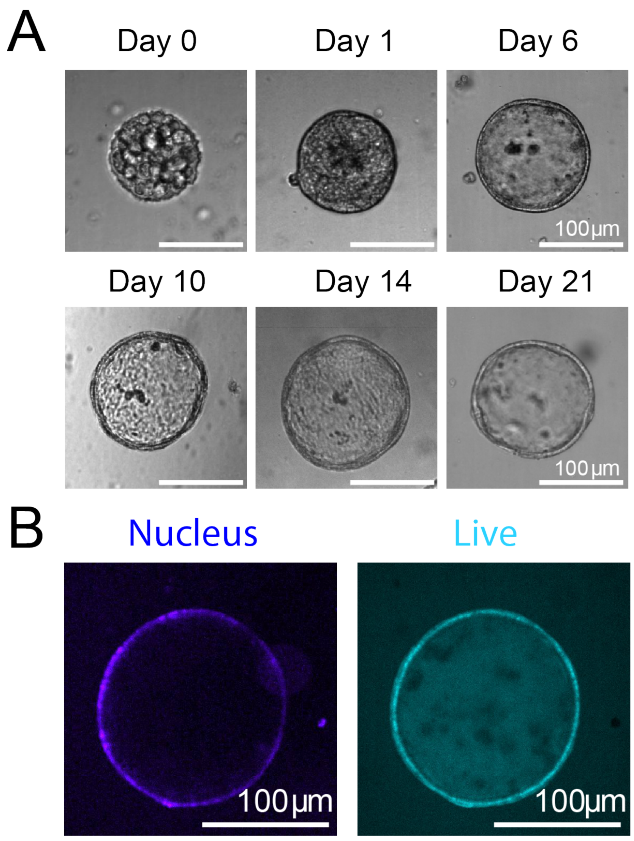

Figure 1.2: A) Representative brightfield confocal images (10X) of Caco-2 cells in agarose microwells (pre-transfer) at day 0 and in a Matrigel matrix (post-transfer) at day 1. Cells self-organize into 120 µm diameter spheroids at day 6 of culture forming a monolayer of cells surrounding a hollow lumen. The spheroids remain viable and lumenized at day 21. B) Live/dead staining assay showing spheroid cell viability after 21 days in culture.

the study of diverse heterotypic cellular interactions characteristic of all metazoan organisms.

1.6 Materials and Methods

Cell culture

Caco-2 cells were maintained in 2D cell cultures as previously described.[31]

Sacrificial Micromolding

Freestanding SU-8 features on silicon wafers were fabricated using photolithographic techniques. Photomasks were designed in AutoCAD and printed by Outputcity Co. Circular

microwells 120 µm in diameter and 80 µm deep were fabricated using SU-8 2035 (MicroChem) spun onto silicon wafers at a speed of 500 rpm for 10 s followed by a 1250 rpm spin for 30 s. The wafer was then soft baked for 5 min at 65°C, for 10 min at 95°C, and UV exposure in contact mode at an energy of 215 mJ/cm^2. Wafers were then postexposure baked for 5 min at 65°C and for 10 min at 95°C, and developed in the SU-8 developer (MicroChem) for at least 20 min. The patterned substrate was then washed with isopropanol/water and hard baked at 150°C for 1 h before measuring pillar heights using a stylus profilometer (Ambios XP2).

This silicon master was used to create PDMS micropillars by pouring a Sylgard 184 (Silicone Elastomer Kit; Dow Corning) onto the patterned wafer using a base:crosslinker ratio of 10:1. After overnight incubation at 65°C, the cured PDMS template was peeled off the silicon master, cut into small rectangular stamps that fit the well of a 24-well plate, and incubated with Sigmacote (Sl-2; Sigma- Aldrich) for several hours to ease the release of the PDMS from the protein-based sacrificial layer. Sacrificial microwells were molded from a solution of 3% (w/v) agarose (Fisher, NH, USA) in phosphate-buffered saline (PBS). This sacrificial agarose mold was generally formed within the wells of a 24-well plate by depositing the PDMS stamp onto a 250 mL drop of liquid agarose. Gelation occurred upon placing the 24-well plate at room temperature for 2 minutes.

To form aggregates, cells were dissociated from culture plates, resuspended in 0.5 mL of media at a concentration of 1×10^6 cells/mL, pipetted onto the imprinted agarose mold in the 24-well plate, and centrifuged into the sacrificial microwells at 160 g at 4°C for 4 min immediately after PDMS removal. Excess cells were then washed away with a medium. To transfer the remaining physically confined cell aggregates from agarose to Matrigel, we carefully pipetted up cell clusters from the microwells and placed them over a 120 mL Matrigel slab (previously set for 30 min at 37°C within the well of a 24-well glass-bottom plate), incubated the dish at 37°C for 1 h and finally overlaid an additional 120 mL of Matrigel on top before adding the media for long-term culture.

Imaging

All confocal microscopy images were acquired using an inverted confocal microscope (Zeiss Cell Observer Z1) equipped with a Yokagawa spinning disk, an Evolve EM- CCD camera (Photometrics), and running NS Elements software.

Live/Dead Staining Assay

The live/dead staining assay was conducted using a 2 mg/ml propidium iodide stock (Sigma-Aldrich Co. LLC, P4170) at a 1:50 dilution and a 5 mg/ml fluorescein diacetate stock (Sigma-Aldrich Co. LLC, C-7521) at a dilution of 1:625 in PBS. As a control or the dead stain, spheroids were fixed using 4% PFA and stained with the live/dead stain.

Chapter 2

Characterization of Human Intestinal Spheroids Cultured using Sacrificial Micromolding

2.1 Introduction

In vitro models of the small intestine that better recapitulate the *in vivo* epithelial barrier are crucial tools to help predict intestinal uptake of drug candidates before costly and laborious animal studies. The 2D monolayer transwell model has been widely used to predict drug permeability across the intestinal epithelial barrier. When cultured on the transwell membrane for 21 days, Caco-2 cells form a tight barrier and spontaneously differentiate to display intestinal enterocyte-like characteristics.[29] However, is it now well-established that 2D models suffer many disadvantages including lack of tissue-specific architecture, cell-cell and cell-matrix interactions, as well as biochemical and mechanical cues.[17] [9] Such interactions with the tissue microenvironment play an important role in determining cell phenotype and functionality, and consequently affect drug transport and drug responses. Hence, there is a crucial need for new *in vitro* models that can recapitulate the complex functions of the human small intestine while efficiently and reliably predicting human responses.

3D cell culture models in which cells are grown within ECM gels are gaining interest for drug discovery and screening as they are thought to induce expression of more tissue-specific function.[44] Matrix effects have been shown to regulate intestinal epithelial differentiation and proliferation. For example, brush border enzyme expression and activity are significantly stimulated while proliferation is slowed down when Caco-2 cells are cultured on a type I collagen or a laminin matrix compared to tissue culture plastic suggesting that integrin-mediated interactions with basement membrane proteins play a crucial role in guiding the intestinal epithelial phenotype.[8] As shown in chapter 1, Caco-2 cells grown in an ECM self-organize into spheroids with a centralized lumen surrounding a monolayer of cells which have the advantages of recreating the spatial organization of intestinal epithelial cells *in vivo*.[15] These

spheroids have physiological cell-cell and cell-matrix interactions and are easily scalable and inexpensive. They, thus, offer the potential to serve as an improved platform for drug discovery and screening that can better simulate intestinal epithelial responses to drugs and stimuli compared to the current 2D monolayer model.

However, the characteristics of these Caco-2 spheroids including their barrier function, potential changes in cell phenotype and transport function brought about by the 3D microenvironment need to be well characterized. Characterization of this model is essential for its application in drug screening as well as studies of epithelial biology.

Here, we report that self-assembling multicellular intestinal spheroids cultured using Sacrificial Micromolding display reproducible intestinal features and functions that are more representative of the *in vivo* small intestine. Additionally, we show that cell polarization and maturation occur faster in spheroids than on transwells and that the spheroids are viable for a longer period of time. Given the simple construction and the ability of the spheroids to reproduce key intestinal features and functions, this system offers the potential to provide readouts that better predict *in vivo* drug permeability than standard 2D cultures while increasing the throughput of drug screening. Moreover, using this model to study the intestinal epithelial barrier could reveal new insights about how therapeutics cross the small intestine *in vivo* and ways in which we can modulate drug transport to increase oral bioavailability of drugs.

Material for this chapter is based on reference[48].

2.2 Self-Organization and Polarization

Polarization of epithelial cells is essential for maintaining their microenvironment and ensuring directional secretion of materials. We compared a small cell aggregate (35 µm in diameter) that did not lumenize to a lumenized 120 µm diameter spheroid. After 5 days in Matrigel, the lumenized spheroids formed a monolayer of cells surrounding a hollow lumen and displayed polarization with a continuous actin belt expressed on the apical membrane facing the lumen. The un-lumenized aggregates did not form a hollow lumen and instead displayed a cell-filled core, lacking the apical actin belt (Fig. 2.1). Figure 2.2B shows a 3D reconstruction of a lumenized spheroid with a confluent cell monolayer and actin lining the perimeter of the apical membrane facing the lumen. The spheroids display brush border formation as shown by ezrin on the apical membrane (Fig. 2.2C). Additionally, β-1 integrin which receives and transduces signals from the ECM and is deeply involved in the epithelial polarization process is shown to be expressed on the basolateral side suggesting engagement with the ECM. E-cadherins are shown to be expressed between cells suggesting cross-communication between cells.

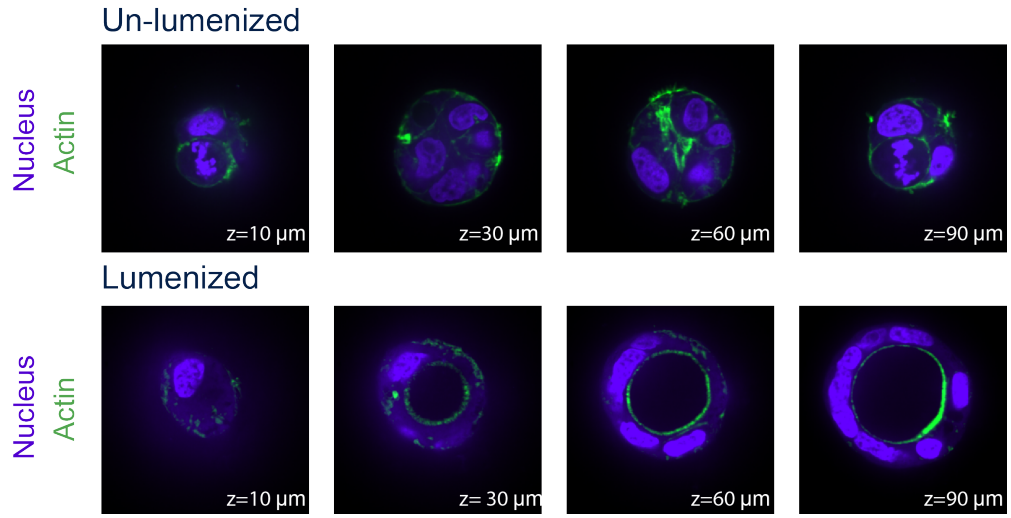

Figure 2.1: Z-stack of lumenized spheroids and un-lumenized aggregates stained with DAPI (blue) and phalloidin (green). Lumenized spheroids display a continuous monolayer of cells surrounding a hollow lumen with an actin belt around the apical membrane whereas un-lumenized aggregates display a cell-filled core, lacking the apical actin belt.

2.3 Barrier Integrity and Transport

To test the barrier function of the spheroids, we first stained for zonula occludens (ZO-1) protein which is one of the essential proteins in the formation of the tight junctional complex in epithelial cells. This barrier limits the diffusion of molecules that are transported via the paracellular route across the small intestine.[2] We showed that the spheroids express ZO-1 co-localized with the actin on the apical membrane of the spheroids (Fig. 2.3A). We also observed that the surface of the intestinal spheroids displays low permeability to high molecular weight dextrans. 2mM 4kDa FITC-dextran was incubated on the basolateral side of lumenized spheroids and un-lumenized aggregates for 3 hours. Figure 2.3B shows that the FITC-dextran was mostly excluded from the lumen of spheroids suggesting a tight epithelial barrier, while the un-lumenized cell aggregate shows penetration of FITC-dextran between the cells. Barrier function of lumenized spheroids was immediately lost by co-incubation with 16 mM EGTA, which serves as a calcium chelating agent and thereby disrupts the tight junctions between the cells.[47] The disruption of tight junctions causes the spheroids to lose their lumenized structure and become leaky allowing for the penetration of FITC-dextran between cells.

Next, we examined the spheroids for efflux pump activity, which is responsible for the active transport of a variety of drugs out of the cells and back into the intestinal lumen, decreasing their oral bioavailability. First, we studied the expression of four highly abundant efflux transporters in the small intestine. P-glycoprotein (Pgp), Breast Cancer Resistance Protein (BCRP), and Multidrug Resistance-associated Protein 2 (MRP2) are responsible

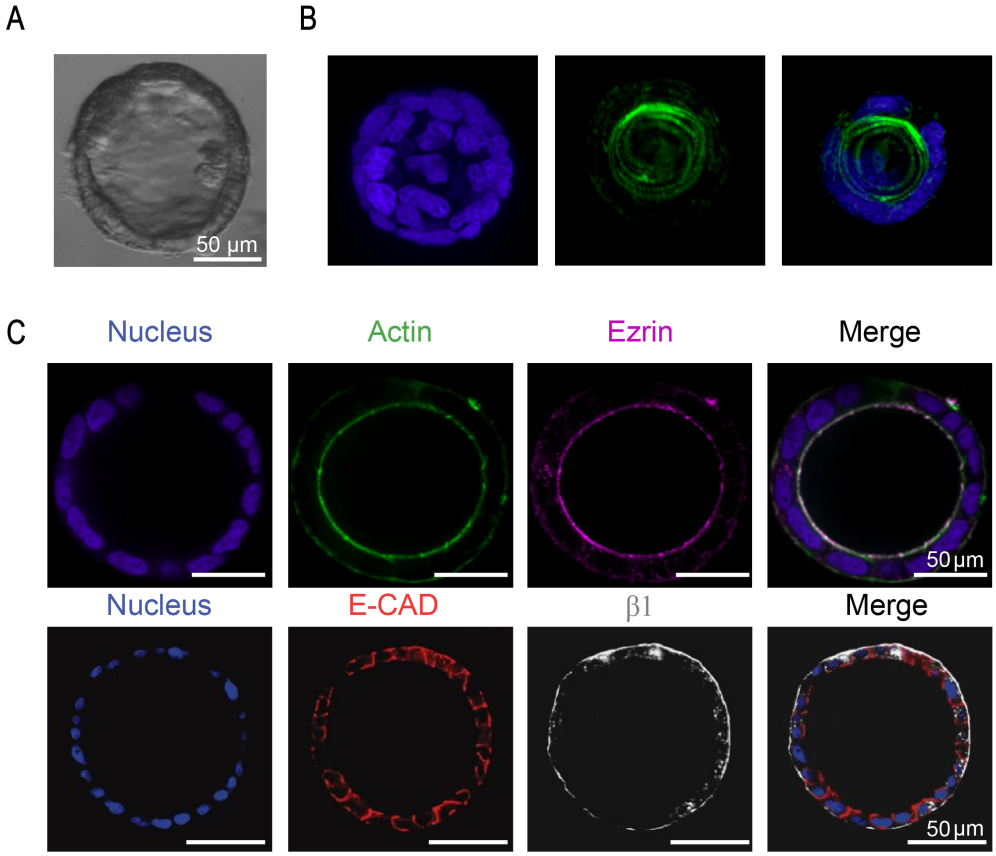

Figure 2.2: Lumenization and polarization of intestinal spheroids after 6 days in culture. A) A representative brightfield confocal image of a lumenized intestinal spheroid at day 6. B) 3D reconstruction of a confocal z-stack showing a representative spheroid forming a confluent monolayer (DAPI) and a continuous actin belt (phalloidin) surrounding the apical membrane. C) Fluorescence images of a brush border shown by ezrin (purple) co-localized with actin (green) on the apical membrane facing the lumen (10X). E-cadherins (red) are forming between cells showing cellular cross-communication while β-1 integrin (grey) is expressed on the basolateral membrane engaging with the extracellular matrix (10X).

for limiting the intestinal absorption and oral bioavailability of many clinically important and frequently prescribed drugs such as immunosuppressants, antibiotics, anticancer drugs, HIV protease inhibitors, and cardiac drugs.[20] We showed that these three transporters are correctly localized on the apical membrane of the spheroids, while Multidrug Resistance-associated Protein 3 (MRP3) is correctly localized on the basolateral membrane (Fig. 2.4). Furthermore, we measured mRNA expression levels of these four transporters after 6 days, 2 weeks, and 3 weeks and found no significant difference in expression levels (Fig. 2.7B ii). This suggests that the spheroids have reached a mature and differentiated state after 6

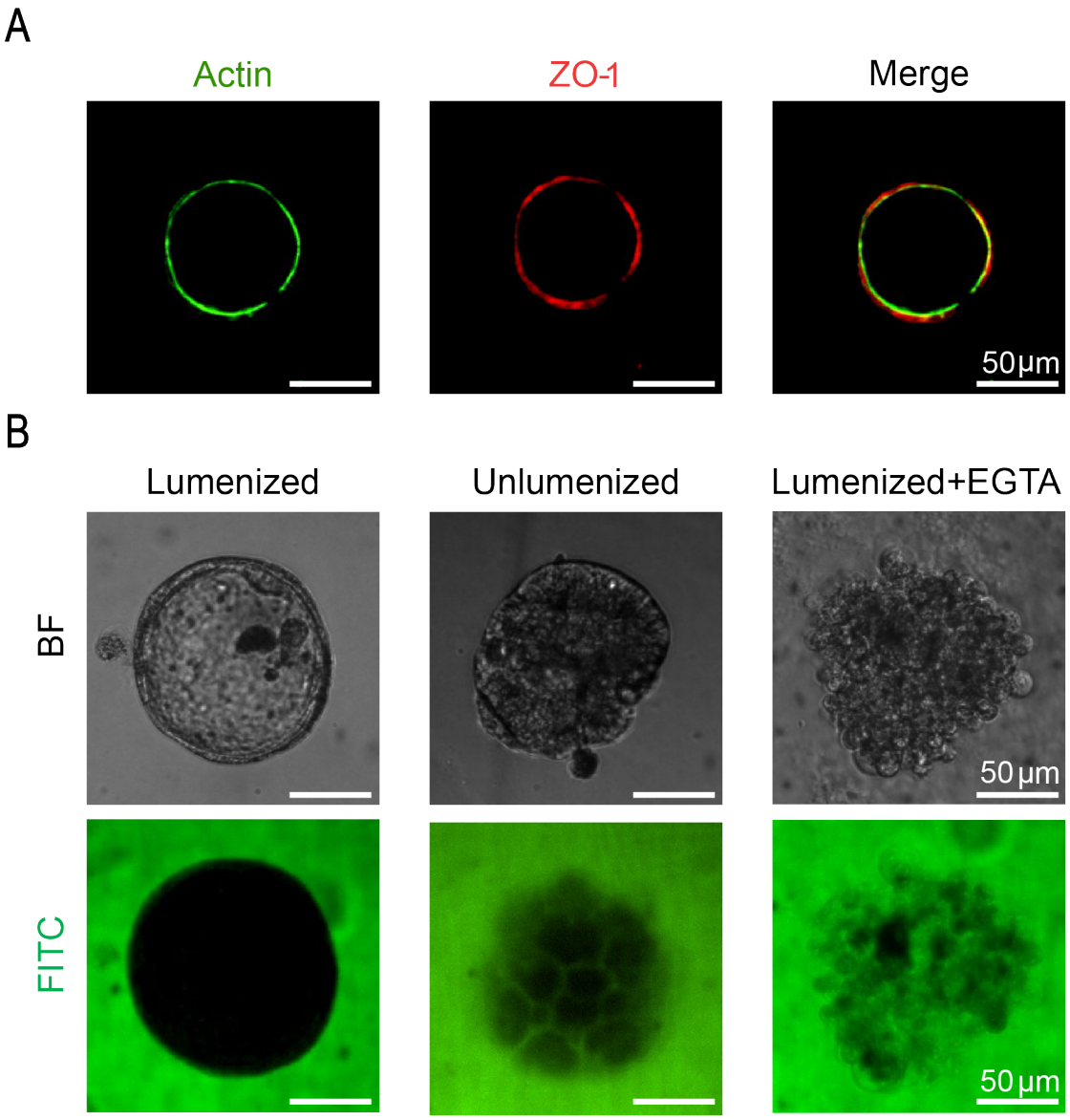

Figure 2.3: Barrier integrity of intestinal spheroids. A) Fluorescent confocal image of a spheroid stained for tight junctional protein ZO-1 (red) expressed on the apical membrane and co-localized with actin (green). B) Barrier integrity assay showing exclusion of 4kDa FITC-dextran after incubation for 3h in a lumenized spheroid while the FITC-dextran penetrates between the cells of an un-lumenized aggregate. Co-incubation of a lumenized spheroid with 16 mM EGTA chelates the tight junctions between the cells.

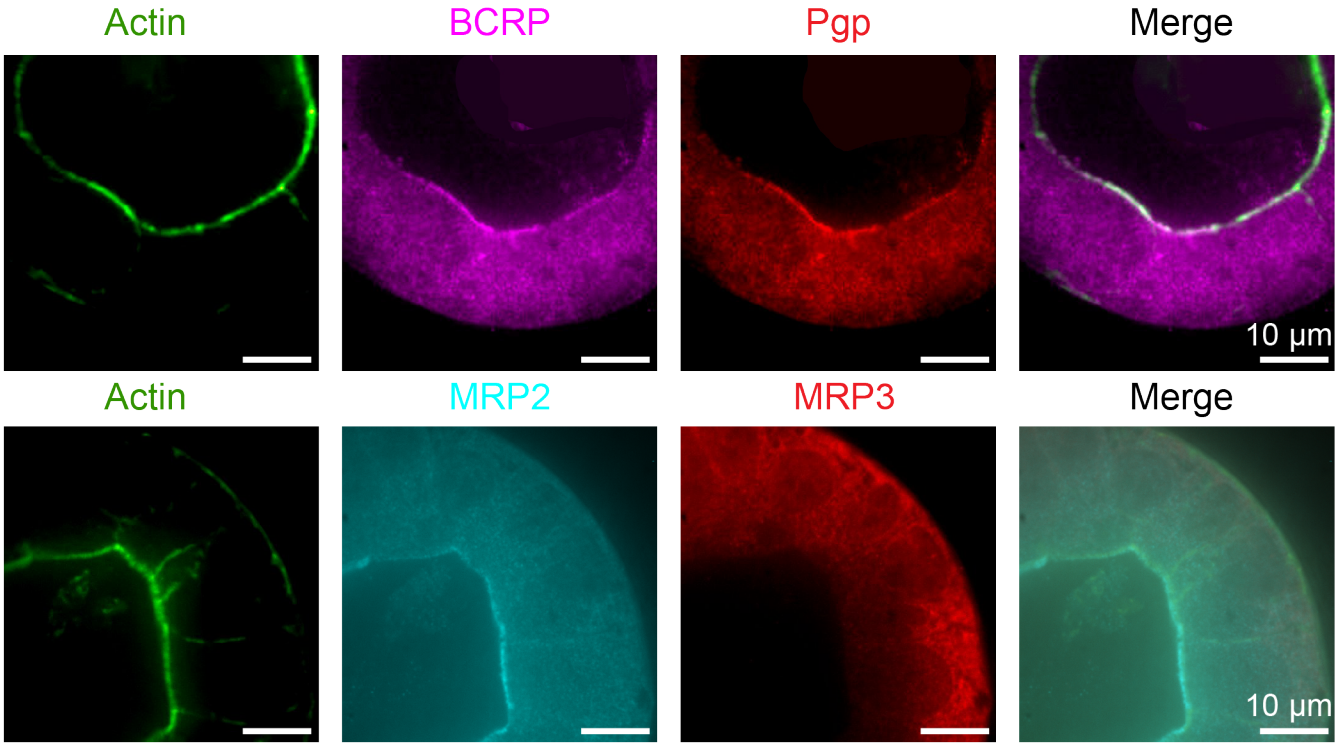

Figure 2.4: Immunofluorescence images showing expression of Pgp (red), BCRP (purple), and MRP2 (cyan) on the apical membrane facing the lumen and MRP3 (red) on the basolateral membrane (60X).

days in culture. As a proof-of-concept, to assess the function of efflux transporters across the spheroids, we used rhodamine 123 (Rh 123) as a model Pgp substrate. When delivered on the basolateral membrane, Rh 123 gets actively transported into the cells.[55] Pgp then actively pumps Rh 123 out of the cell and into the lumen. Upon delivery of 5 µM Rh 123 to the basolateral side of the spheroids, it rapidly accumulated in the apical lumen reaching a concentration of 8 µM within 90 minutes (Fig. 2.5A). However, upon treatment with Cyclosporine A (15 µM), a Pgp inhibitor, Rh 123 accumulated inside the cells and was unable to be transported out into the lumen by Pgp. Previous studies have shown that Rh 123 partitions into the mitochondrial membranes of cells[22] which explains the high fluorescence intensities detected inside the cells upon inhibition of Pgp.

Similarly, we studied the efflux function of BCRP using 5 µM prazosin and 10 µM Methotrexate which are both substrates for BCRP. Upon treatment with the potent inhibitors Ko143 (50 µM) or fumitremorgin C (2 µM), respectively, the luminal concentrations of both drugs decreased significantly (Fig. 2.5B). Taken together, these data suggest that

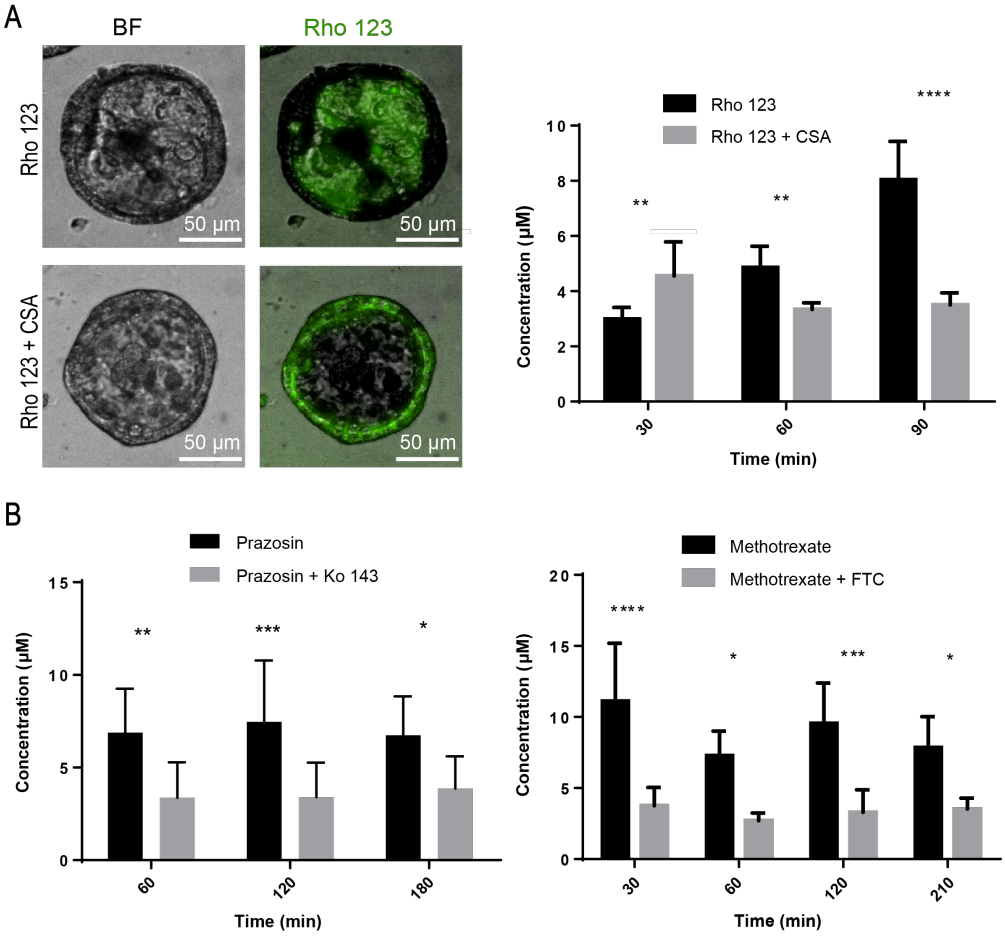

Figure 2.5: Transporter Function. A) Fluorescence images showing Pgp model substrate, Rh 123, accumulating in the lumen of spheroids. Co-incubation with Pgp inhibitor CSA leads to accumulation of Rh 123 inside the cells. Bar graph depicts the influx of Rh 123 into the spheroid (black bars) while the luminal concentration is lower when Rh 123 is co-incubated with CSA (grey bars). The graph shows the mean Rh 123 concentration at different time points. (Mean ± SD; **$p < 0.01$; **** $p<0.0001$, n=10). B) Bar graphs depicting the accumulation of BCRP substrates prazosin and methotrexate inside the lumen (black bars) while the luminal concentration is lower when the spheroids are co-incubated with the BCRP inhibitors Ko143 and FTC, respectively (grey bars). (Mean ± SD; *$p<0.05$; ***$p<0.001$, n=10). Statistical analyses were performed using two-way ANOVA and Sidaks multiple comparison test.

the surface of the spheroids forms a tight barrier expressing functional efflux transporters that limit the absorption of foreign substrates into the spheroid.

2.4 Comparison with the 2D Transwell Model

Since the transwell system is the current gold standard model for intestinal absorption, we compared it to the intestinal spheroid system to characterize the role that the ECM and the 3D architecture play in instructing cellular differentiation and gene expression. The Caco-2 cell line models the phenotypic changes epithelial cells undergo when they migrate along the crypt axis toward the luminal surface. Upon differentiation, Caco-2 cells decrease proliferation by down-regulating genes involved in cell cycle progression and DNA synthesis, while up-regulating genes involved in drug metabolism and transport.[40]

We compared mRNA expression levels of intestinal epithelial differentiation and proliferation markers in the spheroids (grown for 6 days) and monolayers grown on transwell inserts for 21 days (Fig. 5A i). Higher levels of CCND1, the gene encoding cyclin D1 protein, were measured in transwells compared to spheroids. CCND1 is responsible for cell cycle progression in early G1 phase and is a marker for cell proliferation. Inhibition of cyclin D1 in Caco-2 cells has been shown to inhibit cell proliferation and marks a more differentiated phenotype.[18] On the other hand, Glutathione-transferase A 1 (GSTA1) is a Phase II conjugating enzyme that functions in the detoxification of electrophilic compounds, including carcinogens, therapeutic drugs, environmental toxins and products of oxidative stress by conjugation with glutathione. We found the GSTA1 gene to be approximately 6 fold higher in spheroids than in transwells, indicating a more differentiated cell phenotype.[12] This is consistent with previous reports that have shown members of the glutathione S-transferase family to be among the highly induced genes during Caco-2 cell differentiation.[40] Additionally, higher production of apolipoproteins, which are responsible for binding and transport of lipids in the small intestine, is associated with a more differentiated cell phenotype that resembles small intestinal enterocytes more closely.[56] We measured a 2.9 fold increase in APOA1 expression in spheroids compared to transwells. APOA1 is the gene encoding apolipoprotein A-I, a component of high-density lipoprotein (HDL) which is responsible for transporting cholesterol and other phospholipids to the bloodstream. The increased expression of APOA1 again indicates a more differentiated phenotype in spheroids and is consistent with published observations regarding the regulation of apolipoprotein gene expression in enterocytes.[56]

Previous reports have shown that Caco-2 monolayers cultured on transwells for 21 days form a tighter barrier than the human small intestine because of their colonic origin.[1] We measured the gene expression levels of ZO-1 (TJP1) and Occludin (OCLN) in the transwell model compared to the spheroids (Fig. 5A ii). We found that even though the spheroids are more differentiated and develop a more mature intestinal epithelial phenotype, the expression of ZO-1 was 80% lower and Occludin was 60% lower than in transwells. In order to elucidate the role of the ECM in guiding changes in tight junction gene expression lev-

els, we compared monolayers grown on Matrigel coated transwells (0.5 mg/ml Matrigel) to monolayers cultured on the traditional collagen coated transwells (Fig.2.6B). Lower gene expression levels of ZO-1 and occludin were measured on Matrigel coated transwells similar to the spheroids suggesting that these changes might mainly be due to the effect of the ECM proteins. On a biochemical level, brush border enzyme specific activity is commonly used as a marker for intestinal epithelial differentiation. For instance, studies have reported increases in the specific activities of brush border enzymes after culturing Caco-2 cells on different basement membrane proteins. These changes suggest that interactions with basement membrane proteins may promote intestinal epithelial differentiation.[8] The activity of alkaline phosphatase, a digestive enzyme on the apical brush border of intestinal enterocytes, was compared in spheroids and transwells over a period of 3 weeks (Fig. 2.7A iii). After 6 days in culture, activity levels were found to be 2.7 times higher in spheroids. After 14 days, activity levels show 2 fold higher levels in spheroids. No significant difference was detected at 21 days between the two models. These data suggest that when cultured in a 3D environment, Caco-2 cells reach a more mature and differentiated enterocyte-like phenotype over a shorter period of time compared to when cultured on transwells. This further highlights the advantage of using this model for drug screening.

Intestinal transporters play a crucial role in the oral absorption of a wide variety of drugs. Deviations in transporter expression levels between the Caco-2 monolayer model and the human jejunum could potentially result in inaccurate classification of the permeability and intestinal absorption of compounds, especially for drugs whose pharmacokinetics are heavily determined by active transport. We measured a 2.7 fold increase in expression of BCRP in spheroids compared to monolayers cultured on transwells for 21 days (Fig. 2.7B i). Furthermore, MRP3 was downregulated 7.8 fold in spheroids compared to transwells. These trends suggest a more differentiated phenotype that is physiologically more similar to the human jejunum in which BCRP has been shown to be expressed at 1.5-3 fold higher levels and MRP3 at 0.2-0.3 lower levels compared to monolayers on transwells.[42][19] In order to elucidate the role of the ECM in guiding changes in transporter gene expression levels, we again compared transporter expression levels of monolayers grown on Matrigel coated transwells and collagen coated transwells and found no significant difference in transporter gene expression levels. This suggests that these changes are mainly due to the 3D tissue-like architecture of the spheroids (Fig.2.6A).

Furthermore, while spheroid transporter levels did not vary significantly after they reached a mature state at day 6, the transporter expression levels varied from week 1 to week 3 on transwells (Fig. 2.7B ii & iii). This suggests that while Caco-2 cells require 3 weeks of culture on transwells to reach a mature state with a steady expression of transporters, it only takes 6 days for the spheroids to reach a more mature and more biomimetic state. This implies that spheroids will yield consistent and reproducible results if used in the time frame between 6 days and 21 days in Matrigel. This comparison between intestinal spheroids cultured using Sacrificial Micromolding and transwell monolayers highlights the advantages and the substantial potential of this intestinal spheroid platform in facilitating higher-throughput and more robust screening of oral drugs as well as studies of intestinal transport.

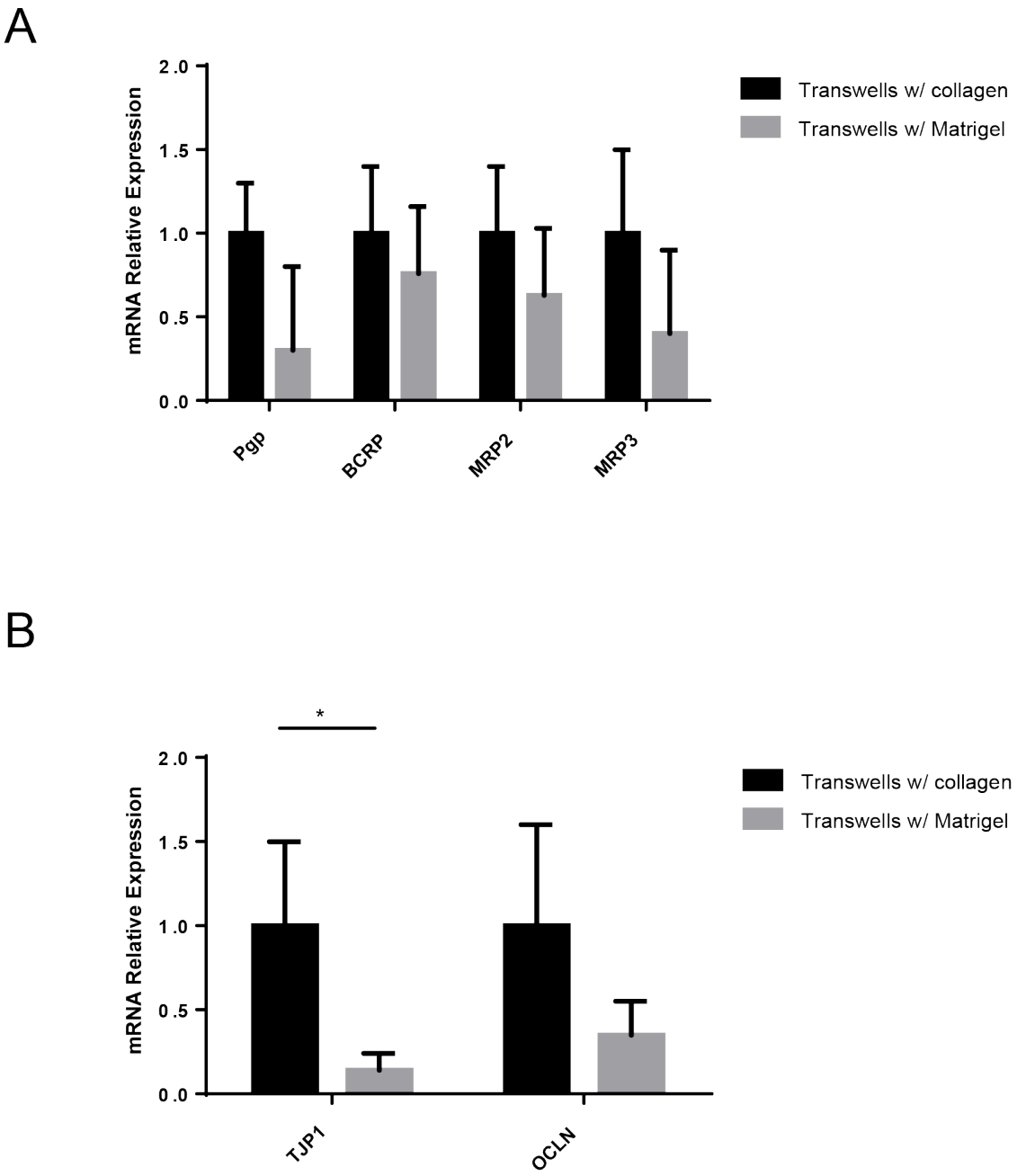

Figure 2.6: Gene expression differences in transporter expression between spheroids and transwells are mainly due to the 3D architecture. A) Comparison between 2D Caco-2 monolayers grown on collagen coated transwells for 3 weeks and monolayers grown on Matrigel coated transwells for 3 weeks showing no significant difference in transporter expression levels. B) Downregulation of ZO-1 and occludin in Matrigel coated transwell monolayers compared to collagen coated monolayers suggesting an important role of ECM protein interactions. (Mean $\pm$ SD; *$p<0.05$; n=3) Statistical analyses were performed using two-way ANOVA with Sidaks or Tukeys multiple comparisons tests.

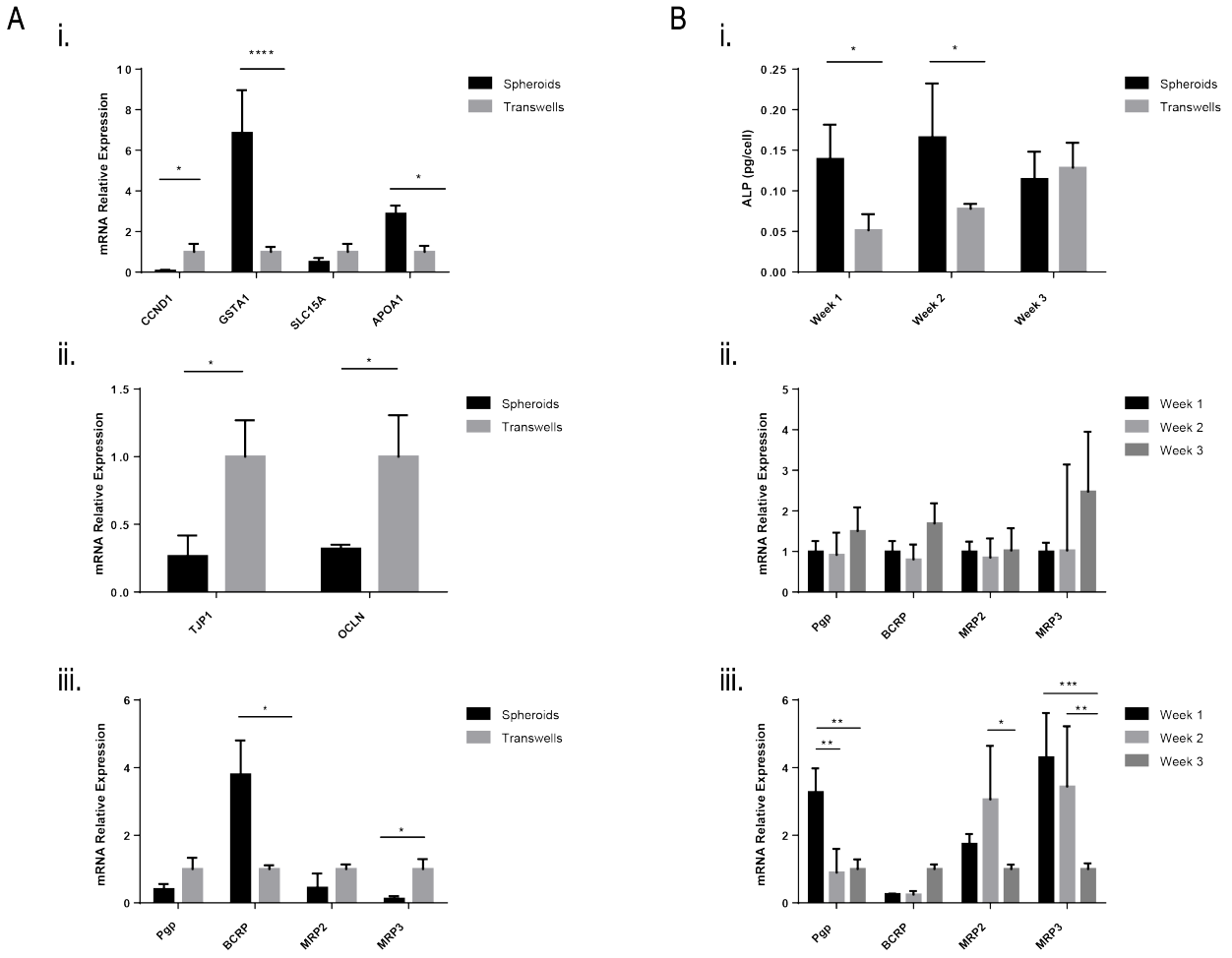

Figure 2.7: A) Comparison between intestinal spheroids at day 6 in culture and monolayers on transwells after 3 weeks in culture showing i.) lower mRNA expression levels of proliferation marker CCND1 and higher expression of differentiation markers GSTA1 and APOA1 in spheroids compared to transwells, ii.) lower expression levels of tight junction proteins TJP1 and OCLN in spheroids, and iii.) more physiological transporter expression levels in spheroids. B) Maturation of spheroids vs. transwells over time. i.) Activity of alkaline phosphatase is higher at week 1 and week 2 in spheroids compared to transwells, ii.) transporter expression remains constant over three weeks in spheroids compared to iii.) significant variations in expression levels in transwells over three weeks. (Mean ± SD; *$p<0.05$; **$p<0.01$; **** $p<0.0001$; n=3) Statistical analyses were performed using two-way ANOVA with Sidaks or Tukeys multiple comparisons tests.

2.5 Summary

Previous research has demonstrated the usefulness of the Caco-2 cell line in predicting drug absorption due to its human origin and its advantageous differentiation into an enterocyte-like phenotype after 21 days on transwells. However, compared to *in vivo* Caco-2 monolayers grown on transwells have a less permeable passive paracellular route, different transporter expression levels, and lower brush border digestive enzyme activity levels. Additionally, in order to expedite the discovery of orally available drugs, methods to shorten the time to reach a fully differentiated confluent Caco-2 cell monolayer are highly desirable.[41] As has been previously shown, moving cells from a 2D to a 3D environment and restoring interactions with the ECM can induce dramatic effects on gene expression, differentiation, and metabolism and can thus more accurately model the *in vivo* phenotype.[52] Here, we showed that Caco-2 spheroids cultured using Sacrificial Micromolding are able to reproduce *in vivo* intestinal epithelial properties and functions after only 6 days in culture. Moreover, a comparison between Caco-2 cells grown on transwells for 3 weeks and spheroids grown for 6 days in an ECM showed that while spheroids do form a tight barrier to high molecular weight dextrans, they display lower tight junction gene expression levels and more physiological transporter expression levels as well as digestive enzyme activity levels. These attributes highlight the spheroid model as a more biomimetic and reproducible intestinal model with potential in facilitating high-throughput screening of oral drugs.

2.6 Materials and Methods

Spheroid Culture

Caco-2 spheroids were cultured using Sacrificial Micromolding as described in chapter 1. Briefly, Caco-2 cells were aggregated in agarose microwells for 24 h before transfer to a Matrigel gel in a glass-bottom 24 well plate in which aggregates were allowed to grow for 5 additional days. Media was refreshed every 2 days.

Transwell Culture

Caco-2 cells (25×10^3 cells/well) were seeded on high density polycarbonate transwell inserts (24-well, 0.4 µm pore size) as previously described.[31] Cells were cultured for 21 days unless otherwise noted. For Matrigel coated transwells, a Matrigel concentration of 0.5 mg/ml was chosen as the highest concentration still enabling the formation of a 2D monolayer. Cells were cultured for 21 days and transepithelial electrical resistance (TEER) was monitored. Only wells with TEER greater than 350 ohm*cm^2 were used for experiments.

Antibody	Product	Dilution
Anti-rabbit Pgp	Abcam 103477	1:50
Anti-rabbit BCRP	Abcam 3380	1:50
Anti-Mouse MRP2	Invitrogen MA-26536	1:50
Anti-rabbit MRP3	Abcam 107083	1:50
Anti-Mouse ZO-1	Invitrogen 339188	1:100
Anti-Rabbit Ezrin	Invitrogen 357300	1:50
Alexa 488 Phalloidin	Life Technologies 1726566	1:500
DAPI	Vector Laboratories H-1200	1:400

Table 2.1: Antibodies and dilutions used for immunohistochemistry.

Immunohistochemistry

Spheroids were fixed with 4% formaldehyde in PBS for 20 minutes followed by incubation in blocking buffer (10% heat-inactivated goat serum in PBS + 0.5% Triton X-100) at 4°C for at least 1 day. After another incubation period of at least 1 day at 4°C with the primary antibody, spheroids were washed several times with PBS and incubated with Alexa-conjugated secondary antibodies (1:200 in blocking buffer) for approximately 1 day. All samples were extensively washed with PBS + Triton X-100 + 1 µg/mL DAPI before imaging. Antibodies used for staining and the dilutions used for immunohistochemistry are included in Table 2.1. Cells were imaged with a Yokagawa CSU22 spinning disk confocal microscope.

Barrier integrity assay

Caco-2 spheroids and Tranwells were incubated in 2mM 4KDa FITC Dextran (Sigma-Aldrich, St. Louis, MO, USA) or 2mM 4kDa FITC Dextran and 16 mM EGTA (Fisher Scientific, Hampton, NH, USA for 3h. Fluorescence intensity in the lumen was measured while keeping laser power and exposure time constant.

Real-time quantitative reverse transcription- polymerase chain reaction

RNA was collected from the 2D culture using the RNeasy Mini kit (Qiagen, Venlo, Netherlands). The 3D aggregates were first extracted from Matrigel by incubating with the Cell Recovery Solution (Corning, Midland, MI, USA) for 2 hours on ice to obtain isolated aggregates, and then RNA was collected with the QIAShredder (Qiagen, Venlo, Netherlands) and RNeasy Mini kit (Qiagen, Venlo, Netherlands). cDNA was generated from the RNA extract with iScript cDNA Synthesis Kit (Bio-Rad, Hercules, CA, USA). qPCR reactions were performed using the SYBR Green PCR Master Mix (Applied Biosystems, Foster City, CA, USA) using L19 as the reference control. Primers sequences used and the proteins they encode are provided in Table2.2.

Gene	Primer Sequence	Protein encoded
MDR1	F 5-GCC AAA GCC AAA ATA TCA GC 3	P-glycoprotein (P-gp)
	R 5-TTC CAA TGT GTT CGG CAT 3	
ABCG2	F 5-TGC AAC ATG TAC TGG CGA AGA 3	Breast cancer resistance protein (BCRP)
	R 5-TCT TCC ACA AGC CCC AGG 3	
ABCC2	F 5-TGA GCA AGT TTG AAA CGC ACAT 3	Multi-resistance protein 2 (MRP2)
	R 5-AGC TCT TCT CCT GCC GTC TCT 3	
ABCC3	F 5-CAC CAA CTC AGT CAA ACG TGC 3	Multi-resistance protein 2 (MRP3)
	R 5-GCA AGA CCA TGA AAG CGA CTC 3	
CCND1	F 5-CAATGACCCCGCACGATTTC 3	Cyclin D1
	R-CATGGAGGGCGGATTTGGAA 3	
SLC15A	F 5-TGTCCACCGCCATCTACCATA 3	Peptide transporter 1 (PEPT 1)
	R 5-CCACGAGTCGGCGATAAGAG 3	
GSTA1	F 5-AGCCGGGCTGACATTCATCT 3	Glutathione-transferase A 1
	R 5-TGGCCTCCATGACTGCGTTA 3	
APOA1	F 5'-CCAAAAAGCAGCTAGTGAAACC 3'	Apolipoprotein A-I
	R 5-AGTTGCAGTGCGGATGGAA 3'	
TJP1	F 5-ACC AGT AAG TCG TCC TGA TCC 3	Zonula Occludin (ZO-1)
	R 5-TCG GCC AAA TCT TCT CAC TCC 3	
OCLN	F 5-CGGG CGA GTC CTG TGA TGA G 3	Occludin
	R 5-TCT TGT ATT CCT GTA GGC CAG T 3	
L19	F 5-TCGCCTCTAGTGTCCTCCG 3	Ribosomal protein
	R 5- GCGGGCCAAGGTGTTTTTC 3	

Table 2.2: Primer sequences used and the name and function of proteins they encode

Alkaline phosphatase detection

Alkaline phosphatase activity was detected with the SensoLyte pNPP ALP Colorimetric Assay Kit (AnaSpec, Fremont, CA, USA) after normalizing cell count with the CyQUANT Cell Proliferation Assay (Invitrogen, Carlsbad, CA, USA). Briefly, cell extracts were collected by incubating either 2D cultures or extracted 3D aggregates in ALP assay buffer with 0.2% Triton-X for 10 minutes at °C, then the solution was spun down at 2500g for 10 minutes and the supernatant was collected as cell extracts. DNA content in the cell extracts were measured with the CyQUANT assay kit to estimate cell numbers in each sample. Reaction volume for each sample was adjusted so that an equal number of cells from each sample was assayed for ALP activity.

Functional efflux assay

Caco-2 spheroids were serum starved for half an hour in serum free EMEM before conducting the transport experiments. Spheroids were incubated with either 5 µM rhodamine 123 (ThermoFisher Scientific, Hampton, NH, USA) or BODIPY FL prazosin (Life Technologies, Carlsbad, CA, USA) or fluorescein methotrexate (Life Technologies, Carlsbad, CA, USA) in serum free EMEM. Inhibition studies were performed by first incubating the spheroids with 15 uM Cyclosporine A (Sigma-Aldrich, St. Louis, MO, USA) or 50 µM Ko 143 (Abcam, Cambridge, UK) or 2 µM fumitremorgin C (Abcam, Cambridge, UK) for 30 minutes at 37°C. After removing the inhibitor solution the spheroids were then incubated with both substrate and inhibitor for 90 minutes. Spheroids were imaged at different time points using a confocal microscope. Fluorescence intensities were measured in the lumen of spheroids while keeping laser power and exposure time constant. Calibration curves of fluorescence intensities vs. drug concentration were used to calculate concentration inside the lumen. All experiments were conducted by taking the average of n=10 spheroids per condition.

Chapter 3

Probing the luminal microenvironment of intestinal spheroids

3.1 Introduction

Emerging 3D culture models facilitate drug testing, tissue engineering, and the study of tissue morphogenesis in a biologically relevant context. Studying the epithelial barrier of 3D Caco-2 spheroids could reveal new insights about how therapeutics cross intestinal barriers *in vivo*. However, the only method for delivering cargo molecules to a 3D lumen is microinjection —a technically complicated method that is intrusive (i.e. must perforate the epithelial barrier), unsuitable for physically large cargo, and inherently low-throughput.[5][6] We, therefore, sought an approach to non-invasively introduce microparticles incorporating drugs or sensors within the lumen of Caco-2 spheroids.

Material for this chapter is based on reference[14].

3.2 Non-intrusive Delivery of Polymeric Microparticles to Intestinal Spheroids

To deliver a microparticle to the interior of a multicellular spheroid, we sought a strategy that would allow small collections of cells to grow and develop around a polymeric microparticle. Based on our analytical model for tissue self-organization[13], we reasoned that the higher affinity of epithelial cells for adhesive ECM relative to a non-adhesive microparticle could direct an aggregate of cells to push a microparticle into their luminal space when fully embedded in adhesive ECM. We, therefore, used Sacrificial Micromolding to pre-aggregate Caco-2 cells and polymeric microparticles within degradable microwells, before transferring

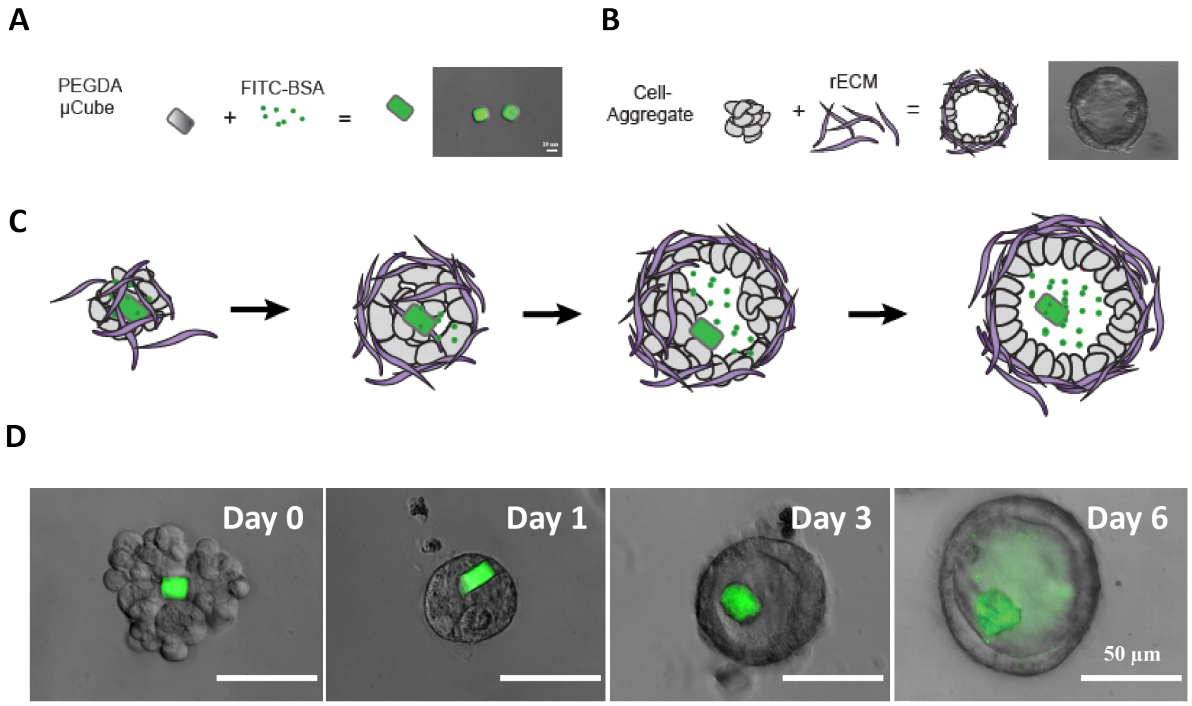

Figure 3.1: Non-intrusive delivery of microparticles to the luminal compartment of a reconstituted spheroid. A) Schematic illustration and 40X image of cuboidal (15 μm 15 μm 15 μm) microparticles made from polyethylene glycol diacrylate (PEGDA) and loaded with FITC-BSA. B) Schematic illustration and 40X phase contrast image of lumenized spheroid reconstituted via Sacrificial Micromolding of a Caco-2 cell-aggregate in Matrigel a reconstituted extracellular matrix (rECM). C,D) Schematic illustration and 40X images of how Sacrificial Micromolding into Matrigel can be used to incorporate the cuboidal PEGDA microparticles into the core of Caco-2 cell-aggregates capable of undergoing morphogenesis, while also retaining the microparticle within the luminal compartment of the spheroid.

these aggregates to Matrigel culture. We initially explored cuboidal microparticles (15 μm X 15 μm X 15 μm) fabricated from polyethylene glycol (PEG) and photolithographically shaped as previously described.[46] Using Sacrificial Micromolding, we found that approximately 25% of the multicellular aggregates that hosted one microcube developed into spheroids incorporating that cube within their lumen, as shown in Fig. 3.1. Using an alternative approach that relied on passive pre-aggregation in non-adhesive microwells and subsequent transfer to Matrigel[13], we found that only 23% of spheroids incorporated the cube within their lumen. Nonetheless, due to i) the high-volume of multicellular aggregates transferred from agarose to Matrigel in each experiment (at least 3000 to 5000), ii) the ease of identifying which aggregates contained microparticles, and iii) the simplicity of the approach, we focused on this latter method for further experimentation.

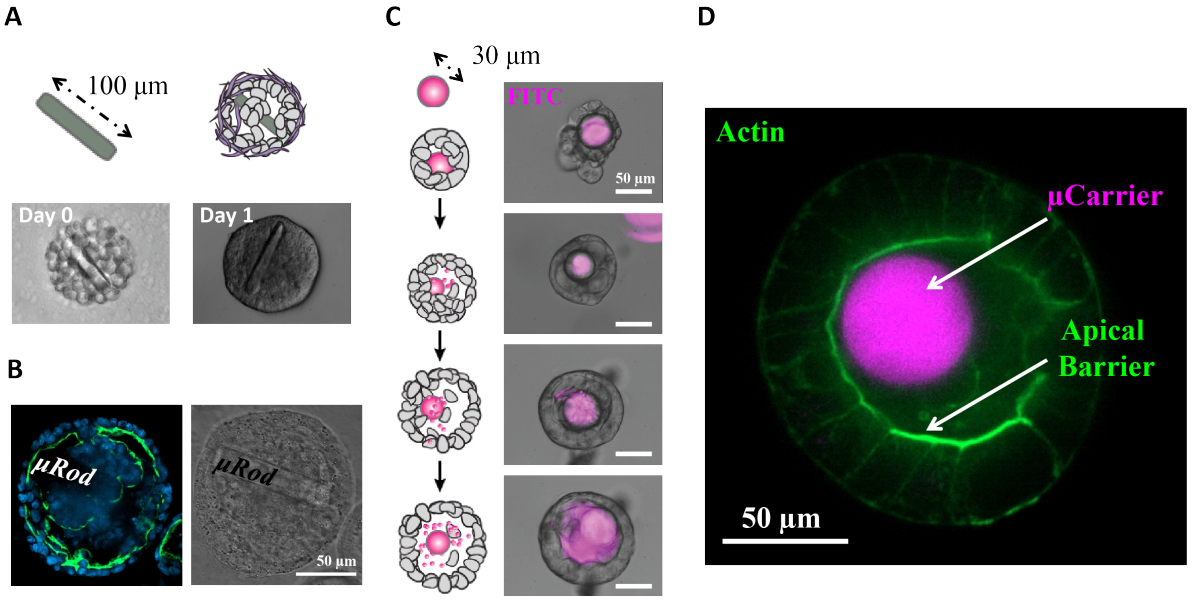

Figure 3.2: Microparticle geometry affects actin belt formation and lumen incorporation. A) Schematic illustration and 40X phase contrast image showing how microrods (15 µm X 15 µm X 15 µm) can be incorporated within the core of Caco-2 microtissues. B) Representative 40X phase contrast image (left) and confocal slice (right) showing how, after one week in culture, microrods alter luminal clearing and the establishment of the characteristic actin belt lining the luminal compartment of a polarized Caco-2 spheroid. C) Schematic illustration (left) and 40X images (right) of PEG microspheres (30 µm in diameter) loaded with FITC-BSA (magenta) and incorporated in lumen. D) 40X confocal slice of a Caco-2 spheroid showing a continuous actin staining signal (green) and a FITC-BSA loaded PEG microsphere (magenta) in the lumen.

3.3 Effect of Microparticle Shape and Size on Actin Belt Formation and Lumenization

During our initial experiments using PEG microcubes, we noticed that slight differences in the size and shape of the cuboidal microparticles appeared to affect lumen formation of reconstituted Caco-2 cells. We, therefore, investigated the effects of microparticle geometry on Caco-2 lumen formation. PEG microrods with dimensions of approximately 15 µm X 15 µm X 10 µm were found too large to be incorporated within multicellular aggregates without affecting lumenogenesis. Even though some microrods could be accommodated within the core of the tissues (Fig. 3.2A), immunofluorescent analysis of actin, a marker of apical polarity, revealed a significant defect in the capacity of these tissues to establish the characteristic actin belt surrounding the lumen of a well-polarized Caco-2 spheroid (Fig.

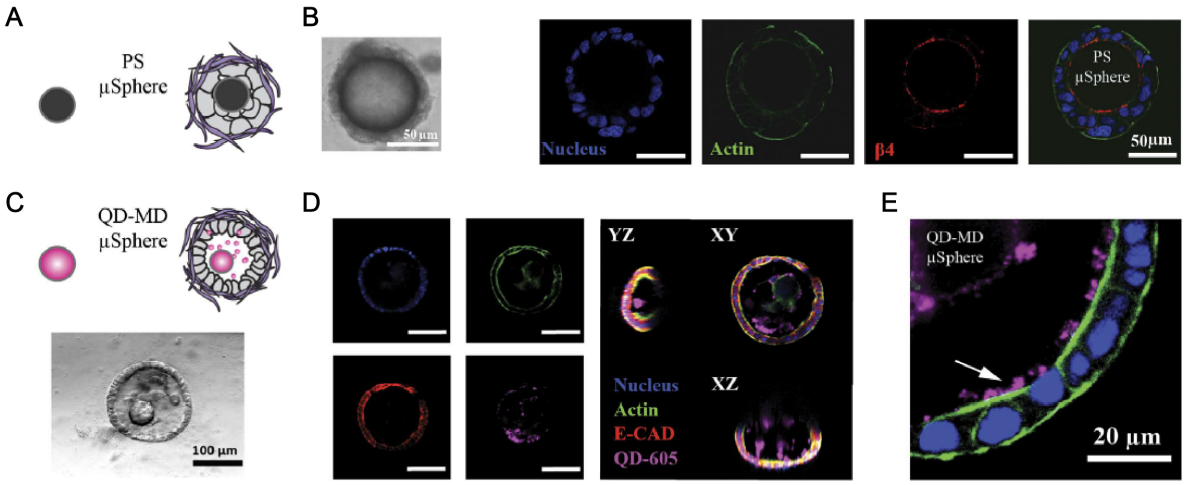

Figure 3.3: Microparticle physicochemical properties affect tissue polarity. A) Schematic illustration (left) and 40X phase contrast image (right) showing polystyrene (PS) microspheres incorporated into the core of Caco-2 microtissues lacking lumen after one week in 3D Matrigel culture. B) 40X confocal slices through a PS microsphere embedded within a Caco-2 cell aggregate and cultured in Matrigel for one week. Caco-2 cells form a coherent microtissue around the microsphere, but the tissue exhibits inverted polarity with actin (green) preferentially oriented towards the surrounding ECM (i.e. Matrigel) and with β-4 integrin (red) localized at the interface between the tissue and the PS-microsphere. Nuclei are stained with DAPI (blue). C) Schematic illustration (top) and 20X phase contrast image (bottom) of a quantum-dot-loaded maltodextrin (QD-MD) microsphere incorporated into the luminal compartment of Caco-2 spheroids after one week in culture. D) 40X confocal slices (left) and 20X confocal orthogonal views (right) of a Caco-2 spheroid with a QD-MD microsphere within its luminal compartment. E) High magnification 63X confocal slice showing quantum dots trapped within the lumen of the spheroid (white arrow).

3.2B). On the other hand, we found that PEG hydrogel microspheres of approximately 30 µm diameter, originally developed as a carrier for drug delivery[3], were more efficient in localizing to the lumen than their cuboidal counterparts (Fig. 3.2C,D), despite their larger volume and surface area. Taken together, these data suggest that differences in size and shape of aggregate-embedded microparticles can have profound effects on lumen formation.

3.4 Effect of Microparticle Composition on Tissue Polarization

We next sought to evaluate the effects of microparticle composition on the capacity of epithelial cells to lumenize. We pre-aggregated Caco-2 cells with either polystyrene (PS) or

maltodextrin microparticles of comparable size and shape. We chose PS because this type of polymer is readily available and routinely used for 3D culture. We chose maltodextrin due to its routine use as an FDA-approved food additive,[26] the simple preparation of maltodextrin microparticles using emulsions,[23] and its capacity to be degraded by secreted intestinal enzymes such as amylase. Unlike PEG microparticles, PS microparticles dramatically perturbed self-organization and spheroid formation as shown in Fig. 3.3A. Although the Caco-2 cells formed coherent microtissues around the microparticles, the basal and apical polarity of these microtissues was completely inverted. β-4 integrin was proximal to the internalized PS microparticle and not in contact with the reconstituted ECM (i.e. Matrigel), while actin appeared to be oriented away from the microparticle itself (Fig. 3.3B). In contrast, bare maltodextrin microparticles and maltodextrin microparticles bearing adsorbed quantum-dots (QD 605) were readily incorporated into Caco-2 spheroids and did not obviously perturb self-organization (Fig. 3.3C). As shown in Fig.3.3D,E, we also found that, after one week in 3D culture, quantum dots had dissociated from the microparticle yet remained completely entrapped within the luminal space of the Caco-2 spheroid, suggesting that the 3D monolayer prevented escape from the luminal compartment. Taken together, these data illustrate delivery of nanoparticle-laden microparticles to the luminal compartment of epithelial spheroids and how the physicochemical properties of the microparticles may trigger undesirable phenomena such as tissue inversion.

3.5 Reversal of Apical-Basal Polarity

We were interested in using our newly found knowledge about the effects of physicochemical properties of microparticles to our advantage. Even though the mechanisms for establishing epithelial polarity are not well understood, it is widely recognized that signals from the ECM are essential for determining the basal membrane and establishing polarity. Additionally, epithelial cells show higher sensitivity to disturbances to apical-basal polarity in 3D culture than in 2D culture conditions.[57]

We wanted to investigate whether we can culture cells around Matrigel beads to intentionally reverse the polarity of the spheroids. We used a flow-focusing microfluidic dropmaker to generate 30-60 µm diameter Matrigel beads (Fig.3.4A). We then pre-aggregated the Matrigel beads with Caco-2 cells in agarose microwells for 24 h and then transferred the cell-bead aggregates to 24-well low adhesion plates for 5 days. Figure 6B shows a Matrigel bead surrounded by cells in an agarose microwell. The cells surround the bead and adhere to the Matrigel forming a monolayer and tight junctions. Using immunostaining, we then showed that indeed the cells displayed an inverted polarity expressing actin on the outer membrane away from the Matrigel bead (Fig.3.4B). Additionally, ZO-1 was co-localized with the actin and expressed on the outer membrane. Inverting the polarity of these spheroids while maintaining a differentiated cell phenotype would be useful in studies of drug transport by allowing access to the apical membrane. This system can be used to conduct further studies of drug transport as well as studies of epithelial polarity.

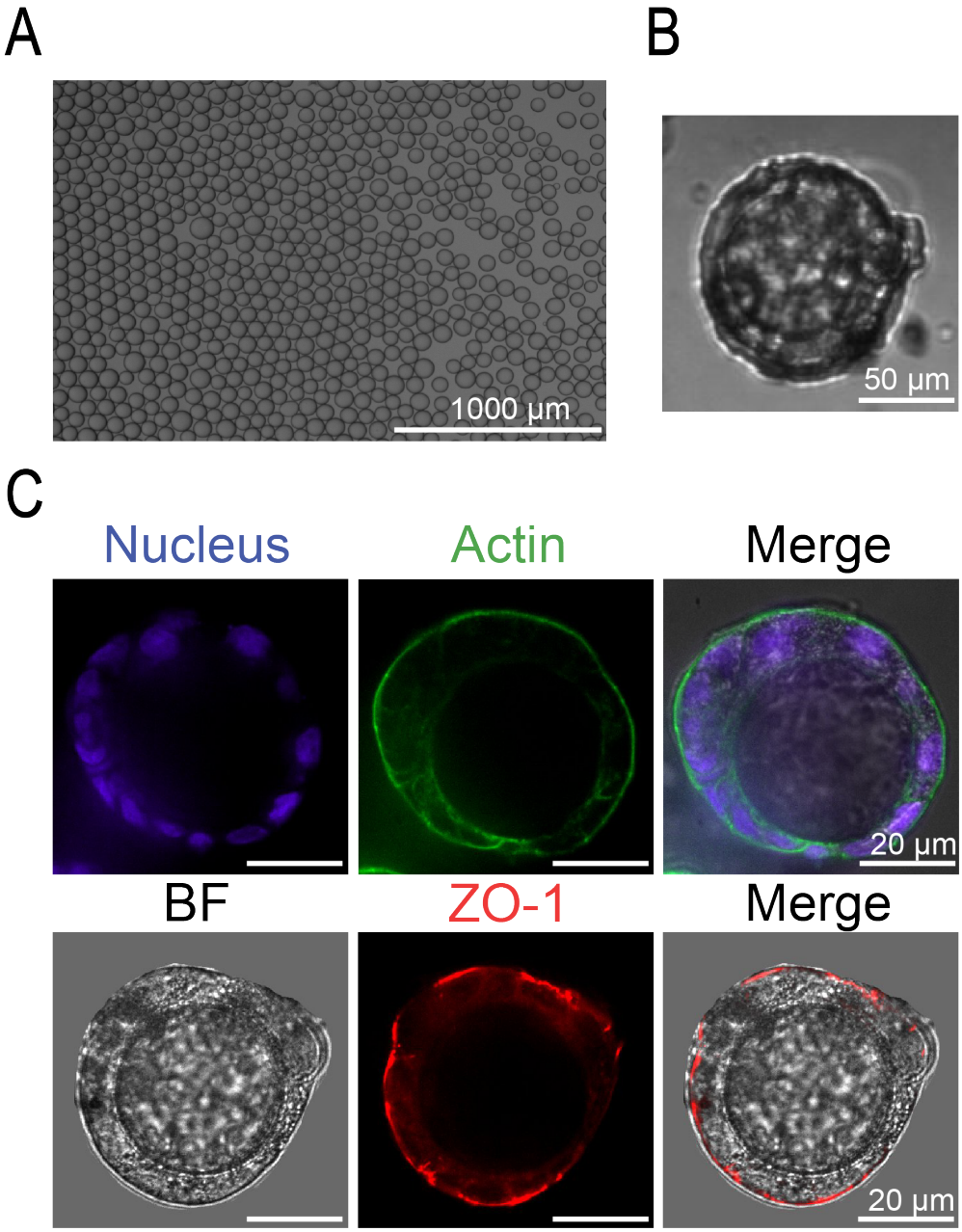

Figure 3.4: Reversal of apical-basal polarity using Matrigel beads. A) Representative image of Matrigel beads in oil (30-60 µm diameter). B) Brightfield image showing Matrigel bead surrounded by cells in an agarose microwell (10X). C) Fluorescent images (40X) showing a continuous monolayer of cells surrounding a Matrigel bead shown by the DAPI stain (blue) and reversal of polarity with actin (green) and tight junction protein ZO-1 (red) expressed on the outer membrane away from the Matrigel bead.

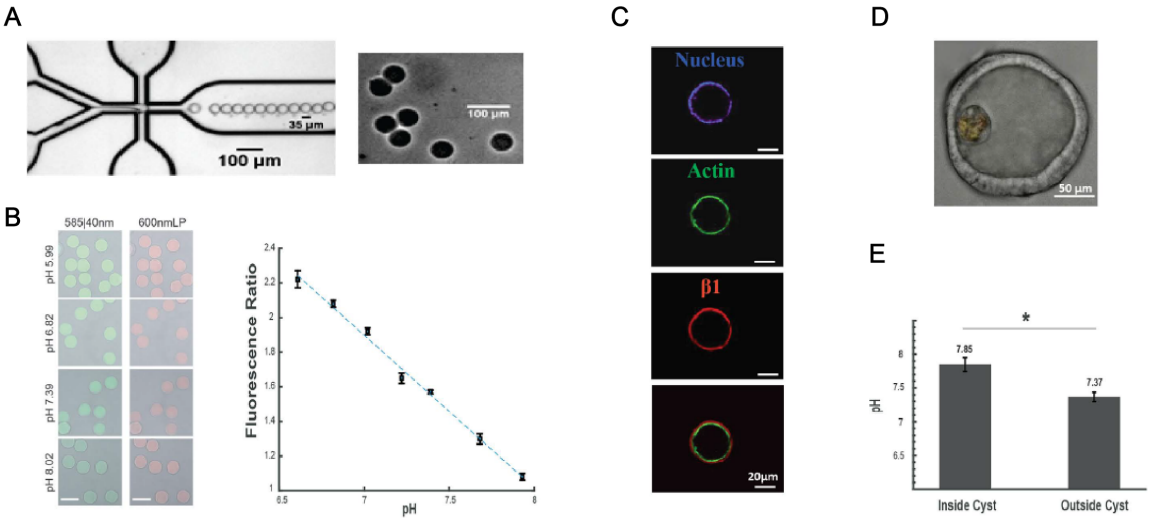

Figure 3.5: Probing the luminal pH of epithelial tissues. A) Sample images of the microfluidic device (left) used to produce 35 µm diameter PEG microparticles that swell to an average diameter of 45 µm in physiological buffers (right). B) Confocal slices showing SNARF-conjugated PEG microparticles with pH-dependent fluorescent profiles (left) and corresponding calibration curve quantifying the ratiometric fluorescent intensity of the microparticles as a function of pH (right). Scale bars are 50 µm. C) 10X confocal slice of a Caco-2 spheroid exhibiting correct basal and apical polarization upon microparticle incorporation. D) Sample 20X image of a Caco-2 spheroid incorporating a SNARF-conjugated PEG microparticle within the luminal compartment and E) quantification of luminal pH within spheroids as opposed to surrounding pH outside spheroids (n = 5) as determined by ratiometric fluorescent intensities of SNARF-conjugated PEG microparticles.

3.6 Polymeric Microsensors Permit the Study of Reconstituted Luminal Microenvironments

Following the successful delivery of nanoparticles to the luminal space of Caco-2 spheroids using degradable microparticles, we sought to further validate our approach by delivering sensors to these lumen. Specifically, we aimed to deliver microsensors capable of characterizing the luminal pH of Caco-2 spheroids with seminaphtharhodafluor (SNARF) - a fluorescent dye used as a ratiometric pH indicator.[38][11] We conjugated SNARF to microparticles constructed from tetra-PEG hydrogel using an adaptation of previously published methods[51] (Fig. 3.5A). Calibration curves for microparticle-conjugated SNARF concentrations between 0.02 and 0.03 mM allowed for ratiometric fluorescent measurements from pH 6.61 to 8.02 in either microparticle or bulk-gel form (Fig. 3.5B). Upon delivering the pH-sensitive microparticle to the luminal compartment of the soheroids, immunofluorescent staining of actin and β-1 integrins indicated correct polarization of the spheroids, suggesting that the non-adhesive

PEG-SNARF microparticles did not affect the self-organization or polarization of these cells (Fig. 3.5C,D). Using the microparticles, we also found that, after one week in culture, the lumen of Caco-2 spheroids exhibited a more alkaline pH than the surrounding medium (Fig. 3.5E); $p < 0.05$ one-way ANOVA). Taken together, these data demonstrate a new approach for luminal delivery of sensors capable of probing the luminal microenvironment of epithelial microtissues.

3.7 Summary

Polymeric microparticles are gaining interest as both drug carriers and sensors. Polymeric sensors can sense specific biological signals, such as release of proteins or antibodies in response to tissue damage and inflammatory events, detect small molecules like glucose and lactose, and monitor pH in real-time and at low concentrations. Despite the advantages of these polymeric sensors to sense biological signals in cellular microenvironments, progress has been limited due to the challenges associated with incorporating these structures into tissues.

We developed a novel method for incorporating polymeric microparticles into the luminal compartment of a reconstituted epithelial spheroid without perturbing tissue self-organization.[50] Using Caco-2 spheroids, we found that small, spherical, and fairly non-fouling polymeric microparticles did not appear to have profound effects on epithelial lumenogenesis. Interestingly, our experiments using PS microparticles did perturb self-organization, yielding microtissues with inverted polarity. It is possible that the rigid and hydrophobic nature of PS may promote the adsorption of secreted ECM molecules and trigger the engagement of cell-ECM adhesion complexes that drive the establishment of this inverted polarity.[58][39] We used this knowledge to our advantage and have shown the potential to reverse the polarity of the spheroids to gain superficial access to the apical membrane by culturing Caco-2 cells around Matrigel beads. We believe that a more extensive characterization of this experimental system is necessary to characterize potential changes in cell phenotype. However, this technique may prove useful experimentally. For example, these spheroids can be incorporated in microfluidic chips to expose the apical membrane to flow to obtain a more physiological system. In contrast, minimally adhesive polymers such as PEG or maltodextrin were better choices for carrier delivery and the study of the luminal microenvironment. In particular, the rich history of PEG as a functionalizable and degradable polymer that can act as a carrier of sensors or therapeutics[28][10][25] makes this material an exquisite choice for future work.

In this proof-of-concept, we use functionalized tetra-PEG hydrogel microparticles to probe the pH of 3D Caco-2 lumen, but we also foresee using degradable PEG microconstructs of increasing complexity in order to non-intrusively deliver therapeutics and other types of nanosensors. For example, there is potential to program tunable and predictable pH-dependent hydrogel degradation and drug-release profiles into PEG microparticles by incorporating cleavable linkers as crosslinks and tethers for drug payloads.[3][49] While the

biological events that allow the internalization of these polymeric microstructures into the lumen of the epithelial spheroids require more detailed investigation, our previous reports suggest that the preferential affinity of epithelial cells for ECM over non-fouling surfaces directs the passive transport of the microparticles away from the ECM interface and towards the spheroid lumen. A more in-depth understanding of this process will be key to the design and development of efficient drug carrier systems and sensors for various applications. However, this study provides a proof-of-concept mechanism of payload delivery into the lumen of Caco-2 spheroids. This paves the way for the possibility of continuous real-time monitoring of analytes within microtissues of increasing complexity, meeting an important need for the field.

3.8 Materials and Methods

Rectangular Microparticles

For a detailed description of how cuboidal or rod-like PEG-microparticles were fabricated via photolithography, see[46] and[45], respectively.

Polystyrene Microparticles, Maltodextrin Microparticles, and Quantum Dot Physisorption

The 75 µm diameter polystyrene beads were purchased from Polysciences Inc (Catalog 24049-5). For maltodextrin microparticles, 2 g of 47 dextrose-equivalent maltodextrin was dissolved in 2 M NaOH. 2 mL of this solution added to 18 mL of 4:1 (v/v) cyclohexane:chloroform with 1% (v/v) Span-80 in a SigmaCote-silanized scintillation vial. This mixture was emulsified by vortexing for 20 seconds, then 400 µL of epichlorohydrin was immediately stirred into the emulsion. The reaction proceeded for 1 hr at 40°C with spinning at 1200 rpm. The emulsion was then washed twice with cyclohexane and four times with distilled water. The resultant polymerized maltodextrin was run through a 100 µm mesh and then a 40 µm mesh to filter out large particles. The beads were assayed for amylase degradability and then used as described. The beads were stored in distilled water at room temperature until use. Quantum dots were loaded onto maltodextrin microparticles by adsorption. Quantum dots (Qdot 605 ITC carboxyl quantum dots, Thermo Fisher) were mixed with 5% of the microparticle prep (equivalent to 100 mg maltodextrin) and incubated overnight in the dark at 4°C in 1 mL of PBS. Microparticles were separated from free quantum dots by centrifugation at 200 g.

SNARF-derivatized Tetra-PEG Hydrogel Microparticles

SNARF-derivatived microparticles were based on biodegradable tetra-PEG hydrogel microparticles originally developed for controlled drug delivery as described in[51]. These gels

self-assemble upon mixing two solutions containing functionalized four-armed PEG prepolymers (Prepolymer A and Prepolymer B), through a strain-promoted azidealkyne cycloaddition (SPAAC) crosslinking reaction. This reaction, also referred to as copper-free click chemistry (see[7]), occurs between four azide (Prepolymer A) and four cyclooctyne (Prepolymer B) end groups to form stable triazole crosslinks between the two tetra-PEG prepolymers. In addition to the azido end-groups used for crosslinking, Prepolymer A also contains free amine end-groups for conjugation to a payload. Here, we attached SNARF to those amino groups, using standard amide-bond-forming chemistry, by acylation with SNARF-NHS ester (Invitrogen S22801) to give a SNARF-functionalized Prepolymer A. Microparticles were formed upon mixing with a solution of the cyclooctyne-derivitized Prepolymer B in a flow-focusing microfluidic drop-forming device (Fig.3.5A).

Cell Culture and Microparticle-cell Mixtures

Caco-2 cells were maintained in 2D cell cultures as described in[31]. After dissociation from culture plates, Caco-2 cells were resuspended in 0.5 ml of EMEM media at a concentration of 1 M cells/ml. The microparticles were added to the cells at a target concentration of 1 microparticle per 100 cells, and 0.5 ml of the particle-cell mixture was pipetted onto the photolithographically defined agarose micromolds before proceeding as described in chapter 1. 3D cell cultures were monitored for lumenization and polarity by phase-contrast, fluorescence, or confocal microscopy as discussed in text.

pH Measurements

SNARF1-functionalized PEG microparticles were suspended in a buffer series from pH 6.61 to 7.93 and imaged on the spinning disk confocal to determine the calibration curve. The ratiometric dye was imaged with a 561 nm laser and fluorescent emission light was collected with a 585/40 nm bandpass filter (f585) and a 600 nm longpass filter (f600). The calibration curve was prepared by calculating the ratio of (f585)/(f600) (Fig.3.5B). Experimental data was collected using the same settings, and the pH of the lumen was determined using the calibration curve obtained for the microparticles in suspension.

Bibliography

[1] P Artursson and J Karlsson. "Correlation between oral drug absorption in humans and apparent drug permeability coefficients in human intestinal epithelial (Caco-2) cells". In: *Biochemical and biophysical research communications* 175.3 (1991), pp. 880–885.

[2] Per Artursson, Katrin Palm, and Kristina Luthman. "Caco-2 monolayers in experimental and theoretical predictions of drug transport". In: *Advanced drug delivery reviews* 46.1-3 (2001), pp. 27–43.

[3] Gary W Ashley et al. "Hydrogel drug delivery system with predictable and tunable drug release and degradation rates". In: *Proceedings of the national academy of sciences* 110.6 (2013), pp. 2318–2323.

[4] Brendon M Baker et al. "Microfluidics embedded within extracellular matrix to define vascular architectures and pattern diffusive gradients". In: *Lab on a chip* 13.16 (2013), pp. 3246–3252.

[5] Sina Bartfeld and Hans Clevers. "Organoids as model for infectious diseases: culture of human and murine stomach organoids and microinjection of Helicobacter pylori". In: *JoVE (Journal of Visualized Experiments)* 105 (2015), e53359.

[6] Sina Bartfeld et al. "In vitro expansion of human gastric epithelial stem cells and their responses to bacterial infection". In: *Gastroenterology* 148.1 (2015), pp. 126–136.

[7] Jeremy M Baskin et al. "Copper-free click chemistry for dynamic in vivo imaging". In: *Proceedings of the National Academy of Sciences* 104.43 (2007), pp. 16793–16797.

[8] Marc D Basson, Gregory Turowski, and Nancy J Emenaker. "Regulation of human (Caco-2) intestinal epithelial cell differentiation by extracellular matrix proteins". In: *Experimental cell research* 225.2 (1996), pp. 301–305.

[9] Mina J Bissell, Aylin Rizki, and I Saira Mian. "Tissue architecture: the ultimate regulator of breast epithelial function". In: *Current opinion in cell biology* 15.6 (2003), p. 753.

[10] Lisa Brannon-Peppas. "Recent advances on the use of biodegradable microparticles and nanoparticles in controlled drug delivery". In: *International journal of pharmaceutics* 116.1 (1995), pp. 1–9.

[11] KJ Buckler and RD Vaughan-Jones. "Application of a new pH-sensitive fluoroprobe (carboxy-SNARF-1) for intracellular pH measurement in small, isolated cells". In: *Pflügers Archiv* 417.2 (1990), pp. 234–239.

[12] Thorsten Buhrke, Imme Lengler, and Alfonso Lampen. "Analysis of proteomic changes induced upon cellular differentiation of the human intestinal cell line Caco-2". In: *Development, growth & differentiation* 53.3 (2011), pp. 411–426.

[13] Alec E Cerchiari et al. "A strategy for tissue self-organization that is robust to cellular heterogeneity and plasticity". In: *Proceedings of the National Academy of Sciences* 112.7 (2015), pp. 2287–2292.

[14] Alec E Cerchiari et al. "Probing the luminal microenvironment of reconstituted epithelial microtissues". In: *Scientific reports* 6 (2016), p. 33148.

[15] Alec Cerchiari et al. "Formation of spatially and geometrically controlled three-dimensional tissues in soft gels by sacrificial micromolding". In: *Tissue Engineering Part C: Methods* 21.6 (2014), pp. 541–547.

[16] Lea Chanson et al. "Self-organization is a dynamic and lineage-intrinsic property of mammary epithelial cells". In: *Proceedings of the National Academy of Sciences* 108.8 (2011), pp. 3264–3269.

[17] Edna Cukierman et al. "Taking cell-matrix adhesions to the third dimension". In: *Science* 294.5547 (2001), pp. 1708–1712.

[18] Qing-Ming Ding, Tien C Ko, and B Mark Evers. "Caco-2 intestinal cell differentiation is associated with G1 arrest and suppression of CDK2 and CDK4". In: *American Journal of Physiology-Cell Physiology* 275.5 (1998), pp. C1193–C1200.

[19] Gunilla Englund et al. "Regional levels of drug transporters along the human intestinal tract: co-expression of ABC and SLC transporters and comparison with Caco-2 cells". In: *European Journal of Pharmaceutical Sciences* 29.3-4 (2006), pp. 269–277.

[20] Margarida Estudante et al. "Intestinal drug transporters: an overview". In: *Advanced drug delivery reviews* 65.10 (2013), pp. 1340–1356.

[21] Ye Fang and Richard M Eglen. "Three-dimensional cell cultures in drug discovery and development". In: *Slas discovery: Advancing Life Sciences R&D* 22.5 (2017), pp. 456–472.

[22] Samantha Forster et al. "Characterization of rhodamine-123 as a tracer dye for use in in vitro drug transport assays". In: *PloS one* 7.3 (2012), e33253.

[23] Gheorghe Fundueanu et al. "Preparation and characterization of starch/cyclodextrin bioadhesive microspheres as platform for nasal administration of Gabexate Mesylate (Foy) in allergic rhinitis treatment". In: *Biomaterials* 25.1 (2004), pp. 159–170.

[24] Andrew P Golden and Joe Tien. "Fabrication of microfluidic hydrogels using molded gelatin as a sacrificial element". In: *Lab on a Chip* 7.6 (2007), pp. 720–725.

[25] Richard B Greenwald et al. "Effective drug delivery by PEGylated drug conjugates". In: *Advanced drug delivery reviews* 55.2 (2003), pp. 217–250.

[26] V Lee Grotz and Ian C Munro. "An overview of the safety of sucralose". In: *Regulatory toxicology and pharmacology* 55.1 (2009), pp. 1–5.

[27] Chin-Lin Guo et al. "Long-range mechanical force enables self-assembly of epithelial tubular patterns". In: *Proceedings of the National Academy of Sciences* 109.15 (2012), pp. 5576–5582.

[28] Jeff Henise et al. "Biodegradable tetra-PEG hydrogels as carriers for a releasable drug delivery system". In: *Bioconjugate chemistry* 26.2 (2015), pp. 270–278.

[29] Ismael J Hidalgo, Thomas J Raub, and Ronald T Borchardt. "Characterization of the human colon carcinoma cell line (Caco-2) as a model system for intestinal epithelial permeability". In: *Gastroenterology* 96.2 (1989), pp. 736–749.

[30] Chris S Hughes, Lynne M Postovit, and Gilles A Lajoie. "Matrigel: a complex protein mixture required for optimal growth of cell culture". In: *Proteomics* 10.9 (2010), pp. 1886–1890.

[31] Kimberly R Kam et al. "Nanostructure-mediated transport of biologics across epithelial tissue: enhancing permeability via nanotopography". In: *Nano letters* 13.1 (2012), pp. 164–171.

[32] Ravi S Kane et al. "Patterning proteins and cells using soft lithography". In: *The Biomaterials: Silver Jubilee Compendium*. Elsevier, 1999, pp. 161–174.

[33] Henning Karlsson et al. "Loss of cancer drug activity in colon cancer HCT-116 cells during spheroid formation in a new 3-D spheroid cell culture system". In: *Experimental cell research* 318.13 (2012), pp. 1577–1585.

[34] Jeffrey M Karp et al. "Controlling size, shape and homogeneity of embryoid bodies using poly (ethylene glycol) microwells". In: *Lab on a Chip* 7.6 (2007), pp. 786–794.

[35] Ali Khademhosseini et al. "Microscale technologies for tissue engineering and biology". In: *Proceedings of the National Academy of Sciences* 103.8 (2006), pp. 2480–2487.

[36] Katie Kingwell. *3D cell technologies head to the R&D assembly line*. 2016.

[37] Hynda K Kleinman et al. "Basement membrane complexes with biological activity". In: *Biochemistry* 25.2 (1986), pp. 312–318.

[38] Oliver Kreft et al. "Polymer microcapsules as mobile local pH-sensors". In: *Journal of Materials Chemistry* 17.42 (2007), pp. 4471–4476.

[39] MP Lutolf and JA Hubbell. "Synthetic biomaterials as instructive extracellular microenvironments for morphogenesis in tissue engineering". In: *Nature biotechnology* 23.1 (2005), p. 47.

[40] John M Mariadason et al. "A gene expression profile that defines colon cell maturation in vitro". In: *Cancer Research* 62.16 (2002), pp. 4791–4804.

[41] Maria Markowska et al. "Optimizing Caco-2 cell monolayers to increase throughput in drug intestinal absorption analysis". In: *Journal of pharmacological and toxicological methods* 46.1 (2001), pp. 51–55.

[42] Nathalie Maubon et al. "Analysis of drug transporter expression in human intestinal Caco-2 cells by real-time PCR". In: *Fundamental & clinical pharmacology* 21.6 (2007), pp. 659–663.

[43] Celeste M Nelson et al. "Emergent patterns of growth controlled by multicellular form and mechanics". In: *Proceedings of the National Academy of Sciences* 102.33 (2005), pp. 11594–11599.

[44] Francesco Pampaloni, Emmanuel G Reynaud, and Ernst HK Stelzer. "The third dimension bridges the gap between cell culture and live tissue". In: *Nature reviews Molecular cell biology* 8.10 (2007), p. 839.

[45] James R Pinney et al. "Discrete microstructural cues for the attenuation of fibrosis following myocardial infarction". In: *Biomaterials* 35.31 (2014), pp. 8820–8828.

[46] James R Pinney et al. "Novel functionalization of discrete polymeric biomaterial microstructures for applications in imaging and three-dimensional manipulation". In: *ACS applied materials & interfaces* 6.16 (2014), pp. 14477–14485.

[47] B Rothen-Rutishauser et al. "Dynamics of tight and adherens junctions under EGTA treatment". In: *The Journal of membrane biology* 188.2 (2002), pp. 151–162.

[48] Karen E Samy et al. "Human intestinal spheroids cultured using Sacrificial Micromolding as a model system for studying drug transport". In: *Scientific reports* 9.1 (2019), p. 9936.

[49] Daniel V Santi et al. "Predictable and tunable half-life extension of therapeutic agents by controlled chemical release from macromolecular conjugates". In: *Proceedings of the National Academy of Sciences* 109.16 (2012), pp. 6211–6216.

[50] Yoshiki Sasai. "Cytosystems dynamics in self-organization of tissue architecture". In: *Nature* 493.7432 (2013), p. 318.

[51] Eric L Schneider et al. "Hydrogel drug delivery system using self-cleaving covalent linkers for once-a-week administration of exenatide". In: *Bioconjugate chemistry* 27.5 (2016), pp. 1210–1215.

[52] Sarah P Short, Patricia W Costacurta, and Christopher S Williams. "Using 3D organoid cultures to model intestinal physiology and colorectal cancer". In: *Current colorectal cancer reports* 13.3 (2017), pp. 183–191.

[53] Temitope R Sodunke et al. "Micropatterns of Matrigel for three-dimensional epithelial cultures". In: *Biomaterials* 28.27 (2007), pp. 4006–4016.

[54] Shauheen S Soofi et al. "The elastic modulus of Matrigelfffdfffdfffd as determined by atomic force microscopy". In: *Journal of structural biology* 167.3 (2009), pp. 216–219.

[55] Matthew D Troutman and Dhiren R Thakker. "Rhodamine 123 requires carrier-mediated influx for its activity as a P-glycoprotein substrate in Caco-2 cells". In: *Pharmaceutical research* 20.8 (2003), pp. 1192–1199.

[56] R DOUG Wagner et al. "Apolipoprotein expression and cellular differentiation in Caco-2 intestinal cells". In: *American Journal of Physiology-Endocrinology and Metabolism* 263.2 (1992), E374–E382.

[57] Shigenobu Yonemura. "Differential sensitivity of epithelial cells to extracellular matrix in polarity establishment". In: *PloS one* 9.11 (2014), e112922.

[58] Wei Yu et al. "β1-integrin orients epithelial polarity via Rac1 and laminin". In: *Molecular biology of the cell* 16.2 (2005), pp. 433–445.